Lattice calculations of nuclear clustering

Dean Lee
Facility for Rare Isotope Beams
Michigan State University
Nuclear Lattice EFT Collaboration

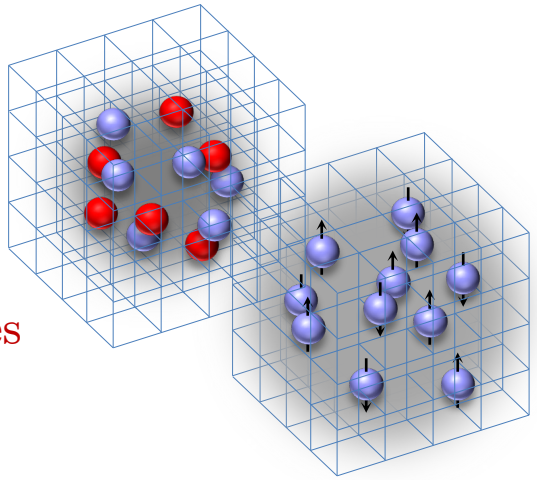

HaloWeek'24 – nuclei at and beyond the driplines
Chalmers University of Technology, Gothenburg
June 9 – 14, 2024

NUCLEI Nuclear Computational Low-Energy Initiative A SciDAC-5 Project

JÜLICH FORSCHUNGSZENTRUM

OAK RIDGE National Laboratory | LEADERSHIP COMPUTING FACILITY

KiSTi www.kisti.re.kr Korea Institute of Science and Technology Information

Outline

Lattice effective field theory

Wavefunction matching

Pinhole algorithm

Relativistic heavy ion collisions

Asymptotic normalization coefficients

Isotopes of beryllium

Isotopes of carbon and oxygen

Summary and outlook

Lattice effective field theory

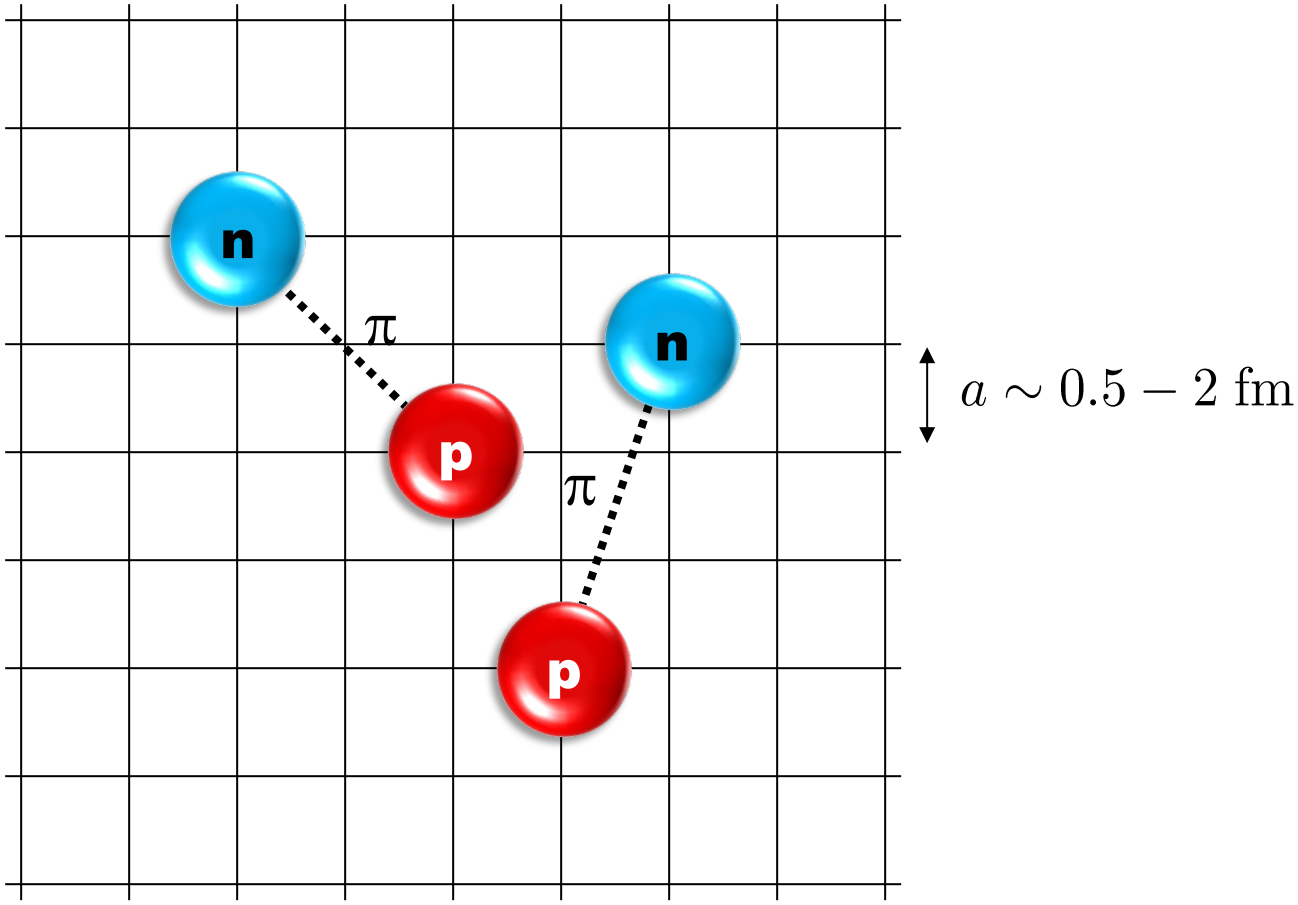

D.L, Prog. Part. Nucl. Phys. 63 117-154 (2009)

Lähde, Meißner, Nuclear Lattice Effective Field Theory (2019), Springer

Chiral effective field theory

Construct the effective potential order by order

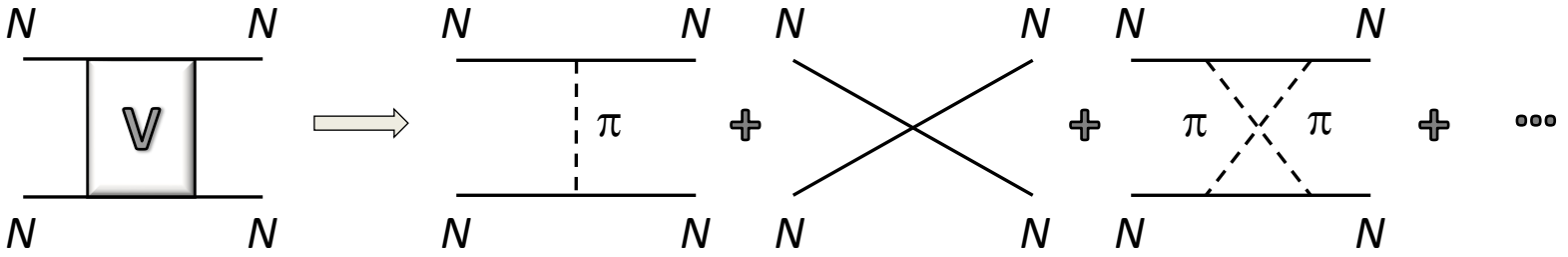

V^{OPEP} Contact interactions V^{TPEP}

Leading order (LO) Next-to-leading order (NLO)

$a = 1.315\,\mathrm{fm}$

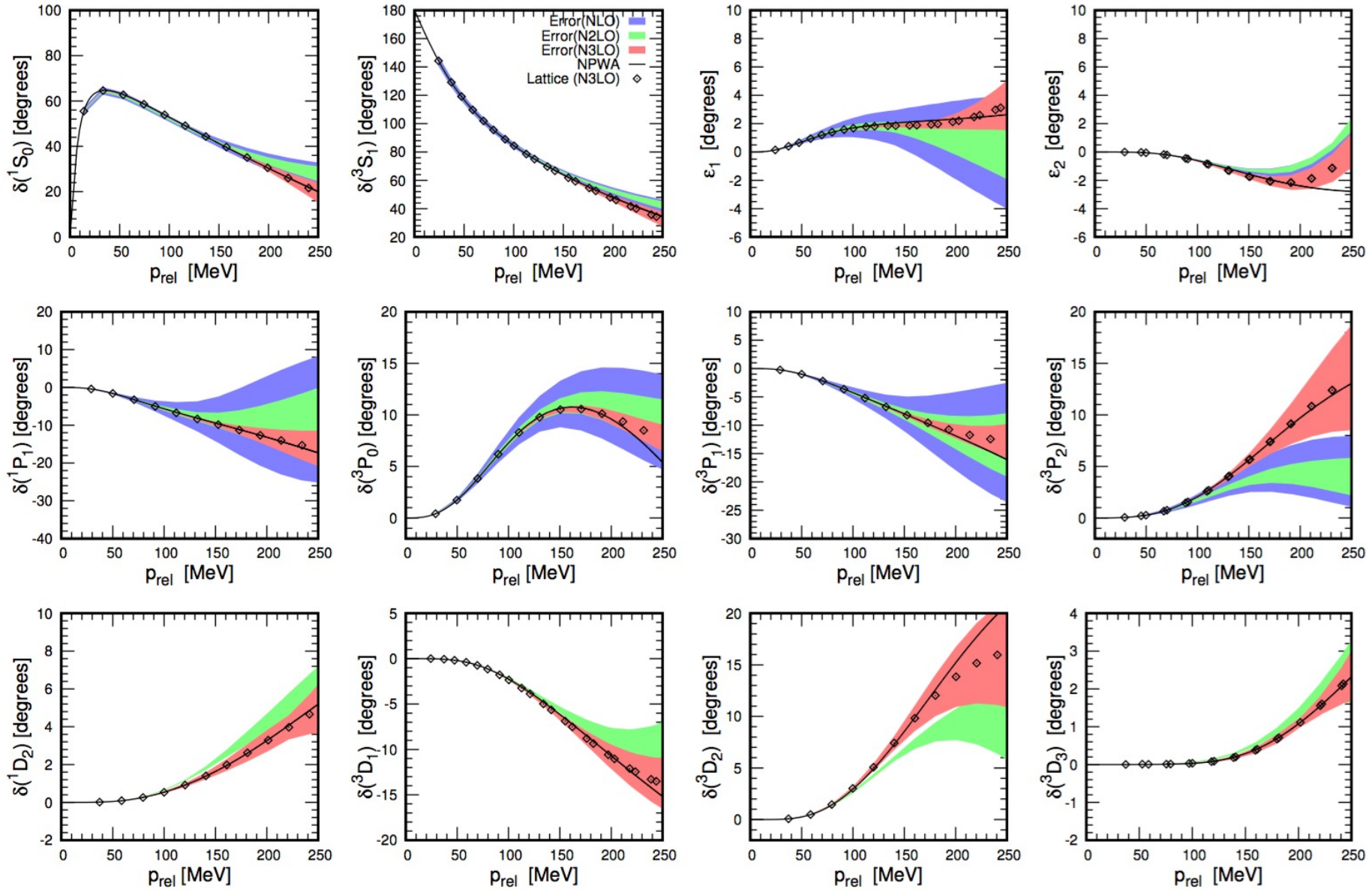

Li, Elhatisari, Epelbaum, D.L., Lu, Meißner, PRC 98, 044002 (2018)

$a = 0.987\,\mathrm{fm}$

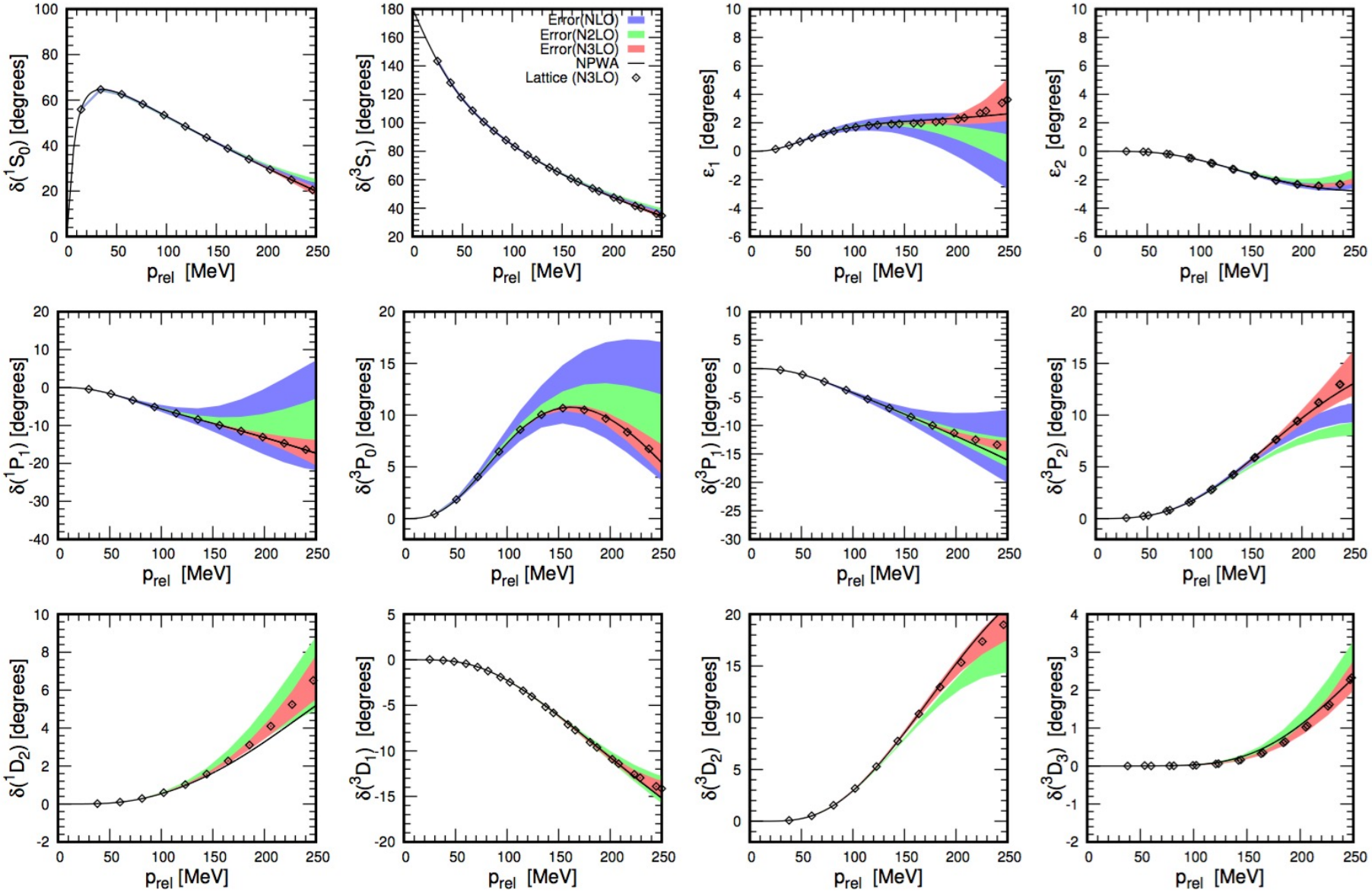

Euclidean time projection

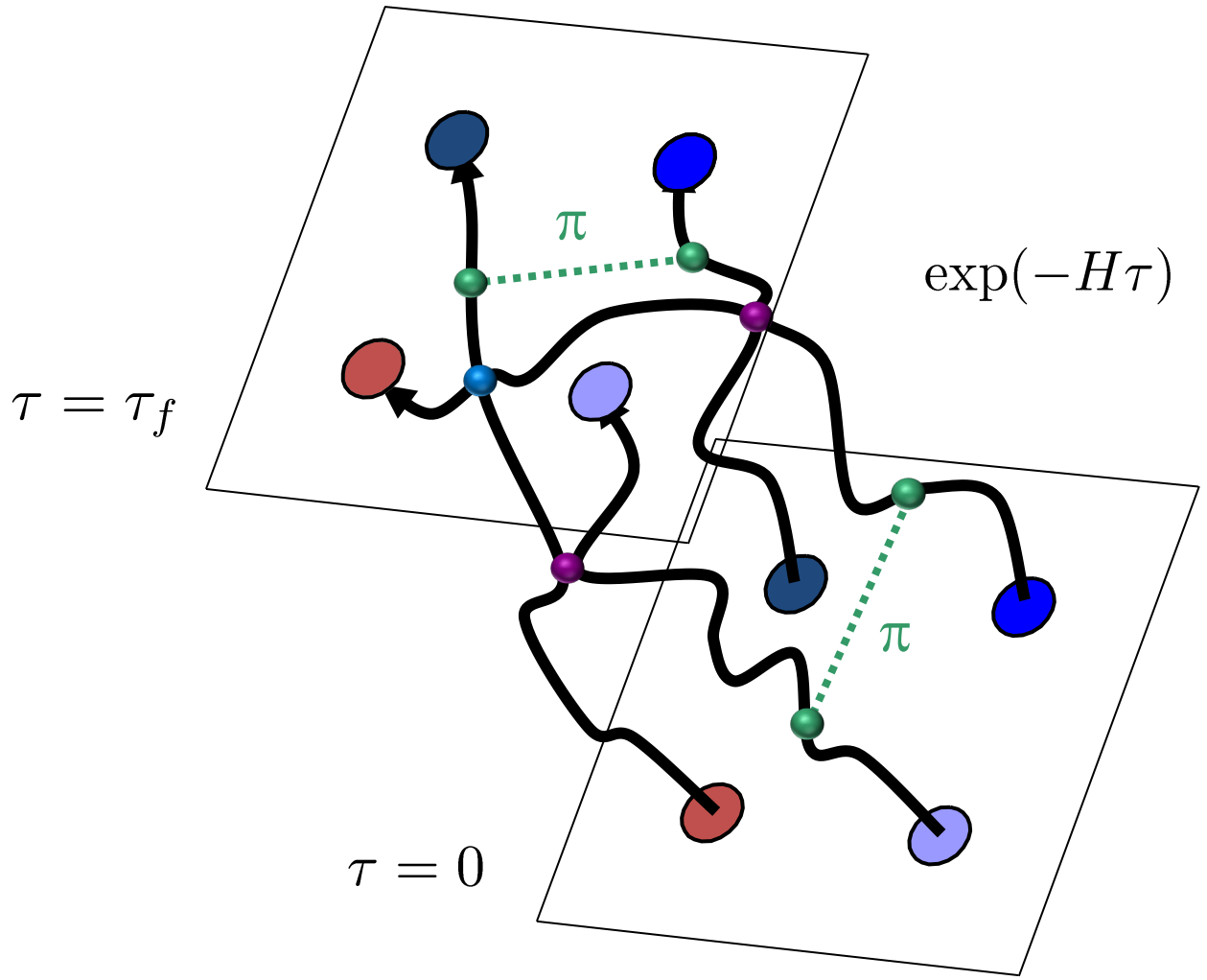

Auxiliary field method

We can write exponentials of the interaction using a Gaussian integral identity

$$\exp\left[-\frac{C}{2}(N^\dagger N)^2\right] \qquad \times \quad (N^\dagger N)^2$$

$$= \sqrt{\frac{1}{2\pi}}\int_{-\infty}^{\infty} ds \exp\left[-\frac{1}{2}s^2 + \sqrt{-C}\, s(N^\dagger N)\right] \qquad \rightarrow \quad sN^\dagger N$$

We remove the interaction between nucleons and replace it with the interactions of each nucleon with a background field.

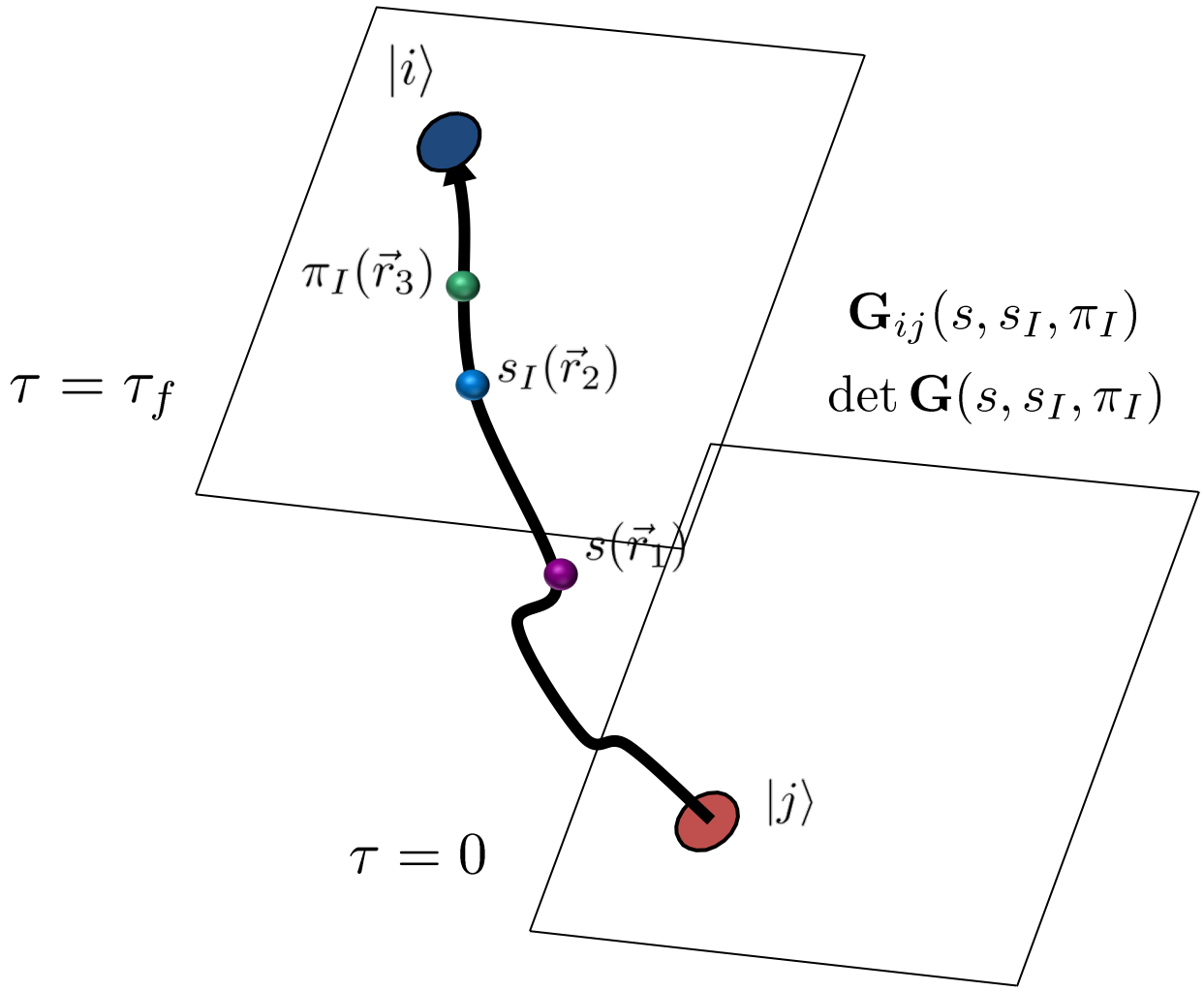
$|i\rangle$
$\pi_I(\vec{r}_3)$
$s_I(\vec{r}_2)$
$s(\vec{r}_1)$
$|j\rangle$
$\tau = \tau_f$
$\tau = 0$
$\mathbf{G}_{ij}(s, s_I, \pi_I)$
$\det \mathbf{G}(s, s_I, \pi_I)$

Wavefunction matching

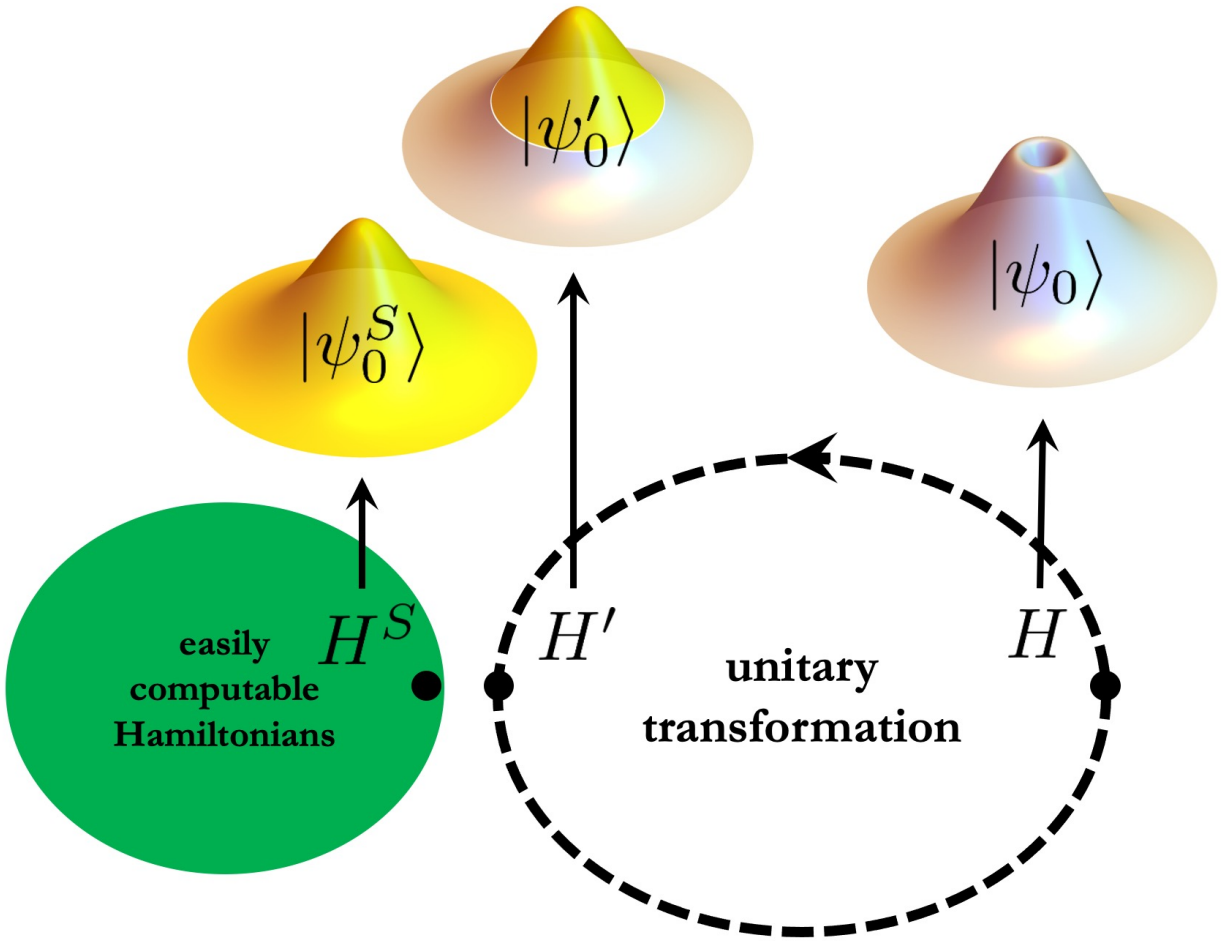

Elhatisari, Bovermann, Ma, Epelbaum, Frame, Hildenbrand, Krebs, Lähde, D.L., Li, Lu, M. Kim, Y. Kim, Meißner, Rupak, Shen, Song, Stellin, Nature 630, 59 (2024)

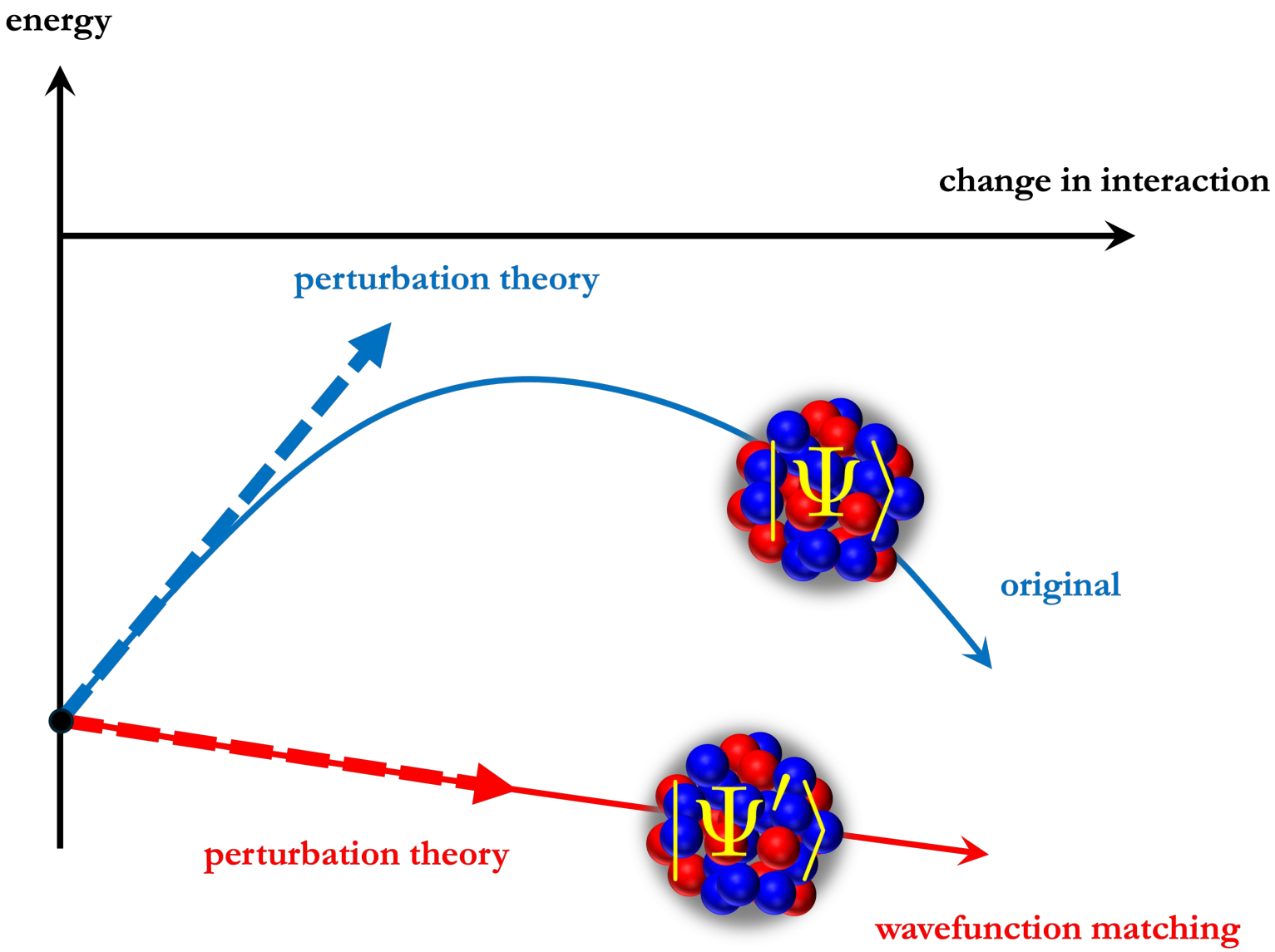
energy
change in interaction
perturbation theory
original
perturbation theory
wavefunction matching

Ground state wavefunctions

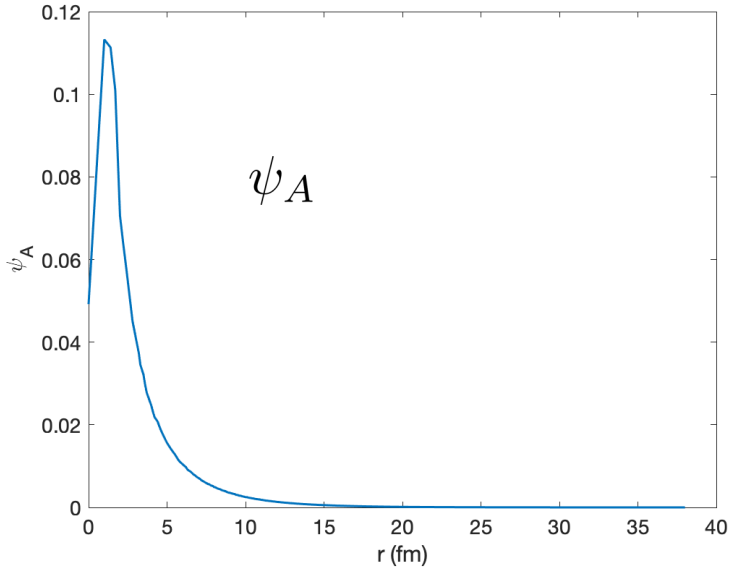

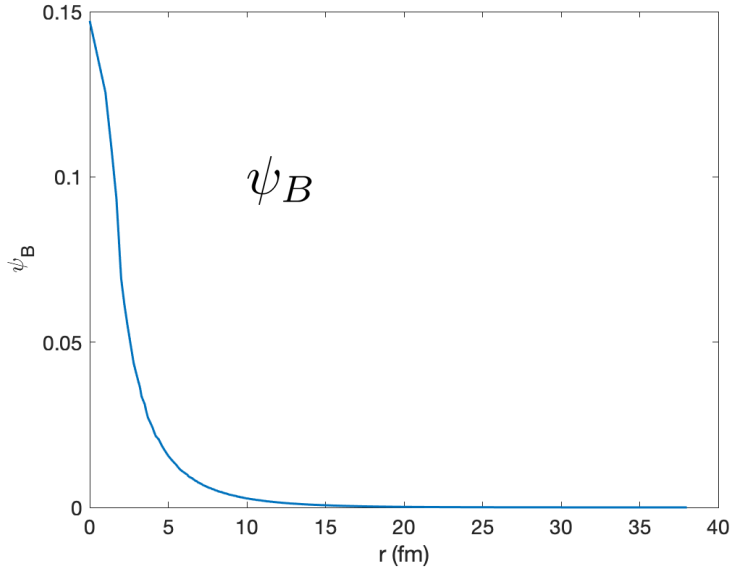

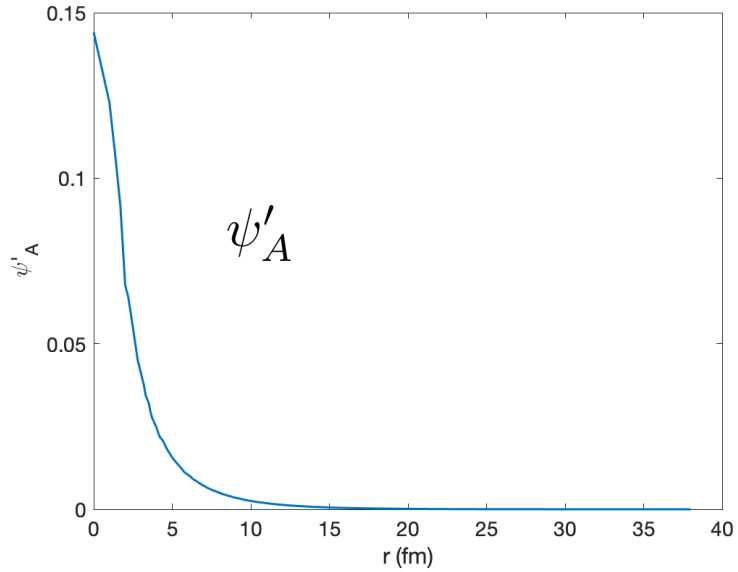

With wavefunction matching, we can now compute the eigenenergies starting from the eigenfunctions of H_B and using first-order perturbation theory.

$E_{A,n} = E'_{A,n}$ (MeV)	$\langle\psi_{B,n}\|H_A\|\psi_{B,n}\rangle$ (MeV)	$\langle\psi_{B,n}\|H'_A\|\psi_{B,n}\rangle$ (MeV)
-1.2186	3.0088	-1.1597
0.2196	0.3289	0.2212
0.8523	1.1275	0.8577
1.8610	2.2528	1.8719
3.2279	3.6991	3.2477
4.9454	5.4786	4.9798
7.0104	7.5996	7.0680
9.4208	10.0674	9.5137
12.1721	12.8799	12.3163
15.2669	16.0458	15.4840

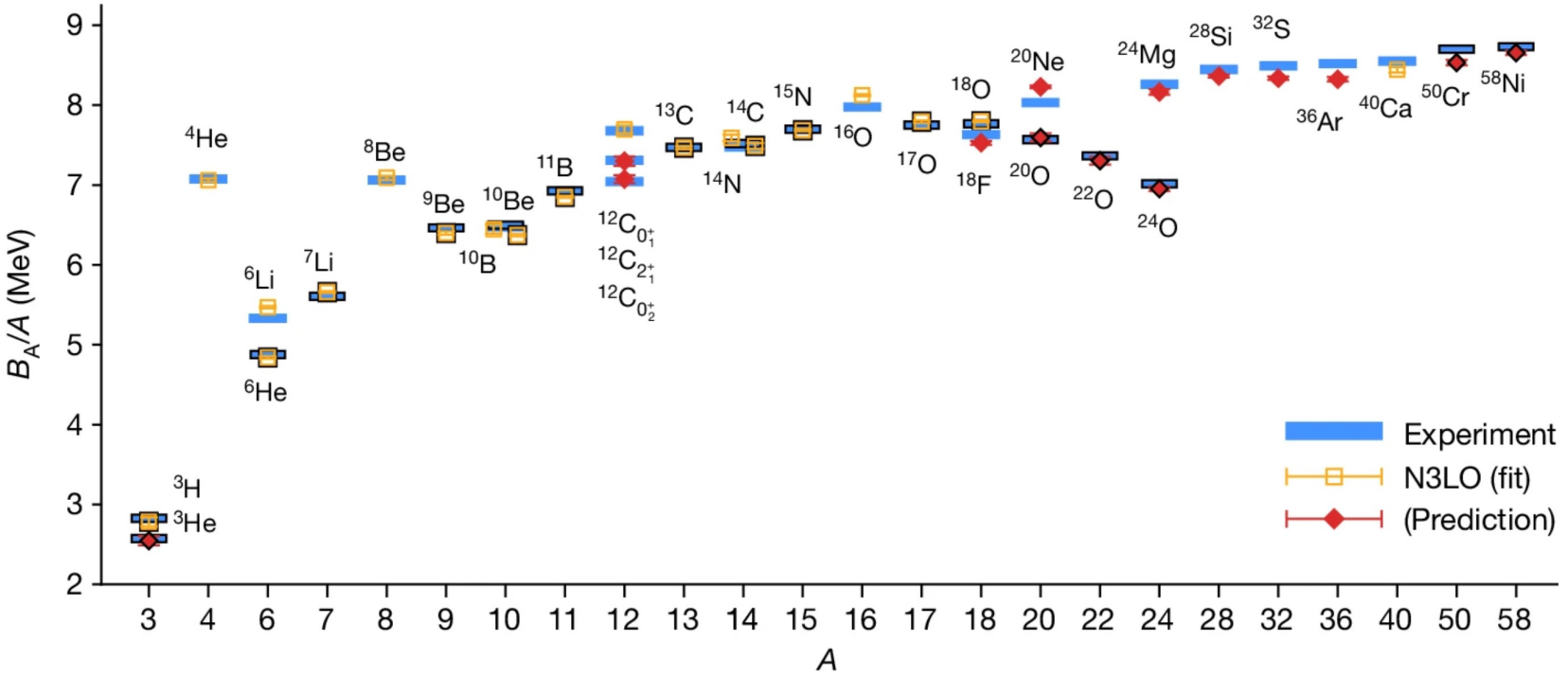

Elhatisari, Bovermann, Ma, Epelbaum, Frame, Hildenbrand, Krebs, Lähde, D.L., Li, Lu, M. Kim, Y. Kim, Meißner, Rupak, Shen, Song, Stellin, Nature 630, 59 (2024)

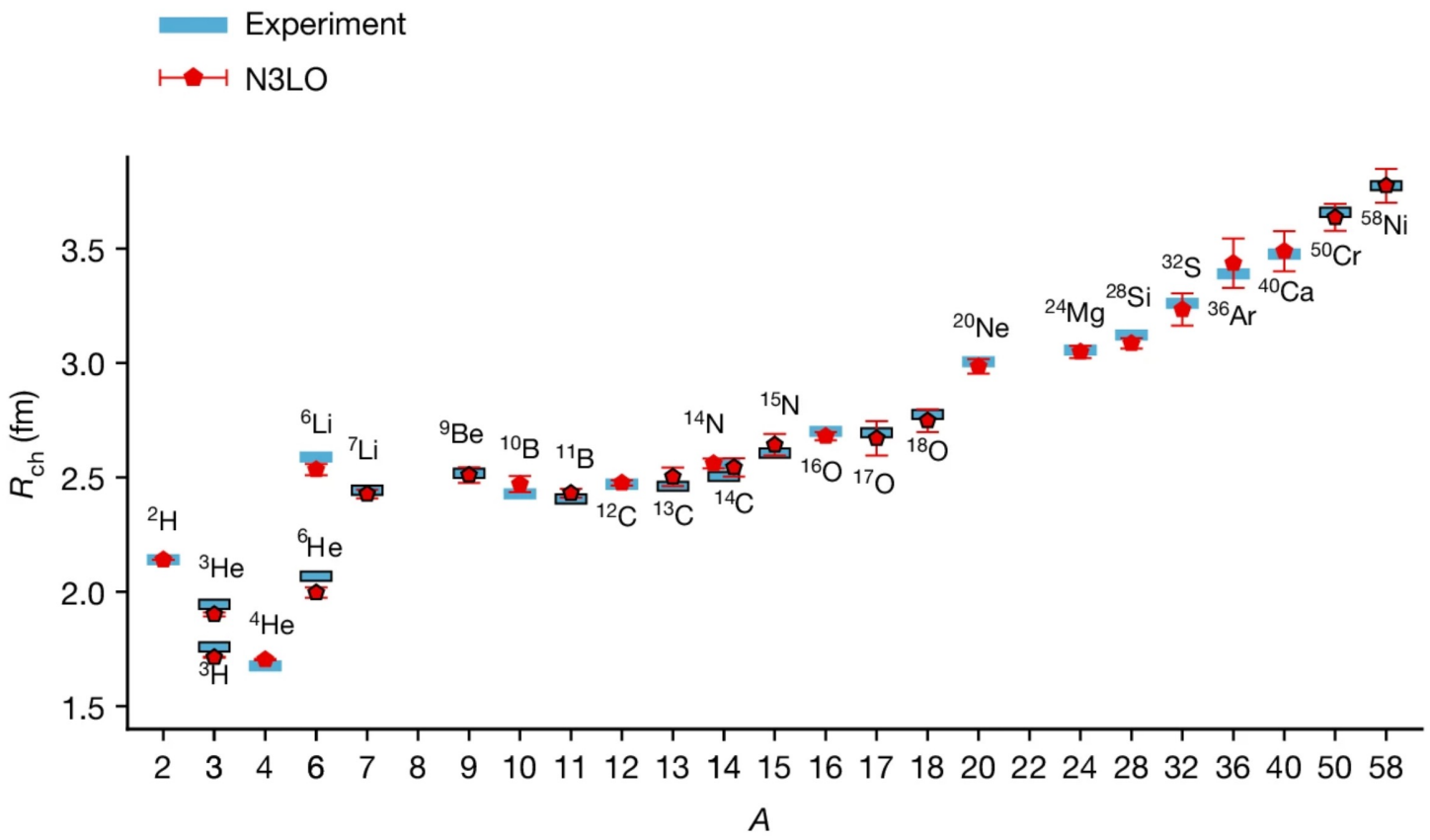

Elhatisari, Bovermann, Ma, Epelbaum, Frame, Hildenbrand, Krebs, Lähde, D.L., Li, Lu, M. Kim, Y. Kim, Meißner, Rupak, Shen, Song, Stellin, Nature 630, 59 (2024)

Silicon isotopes

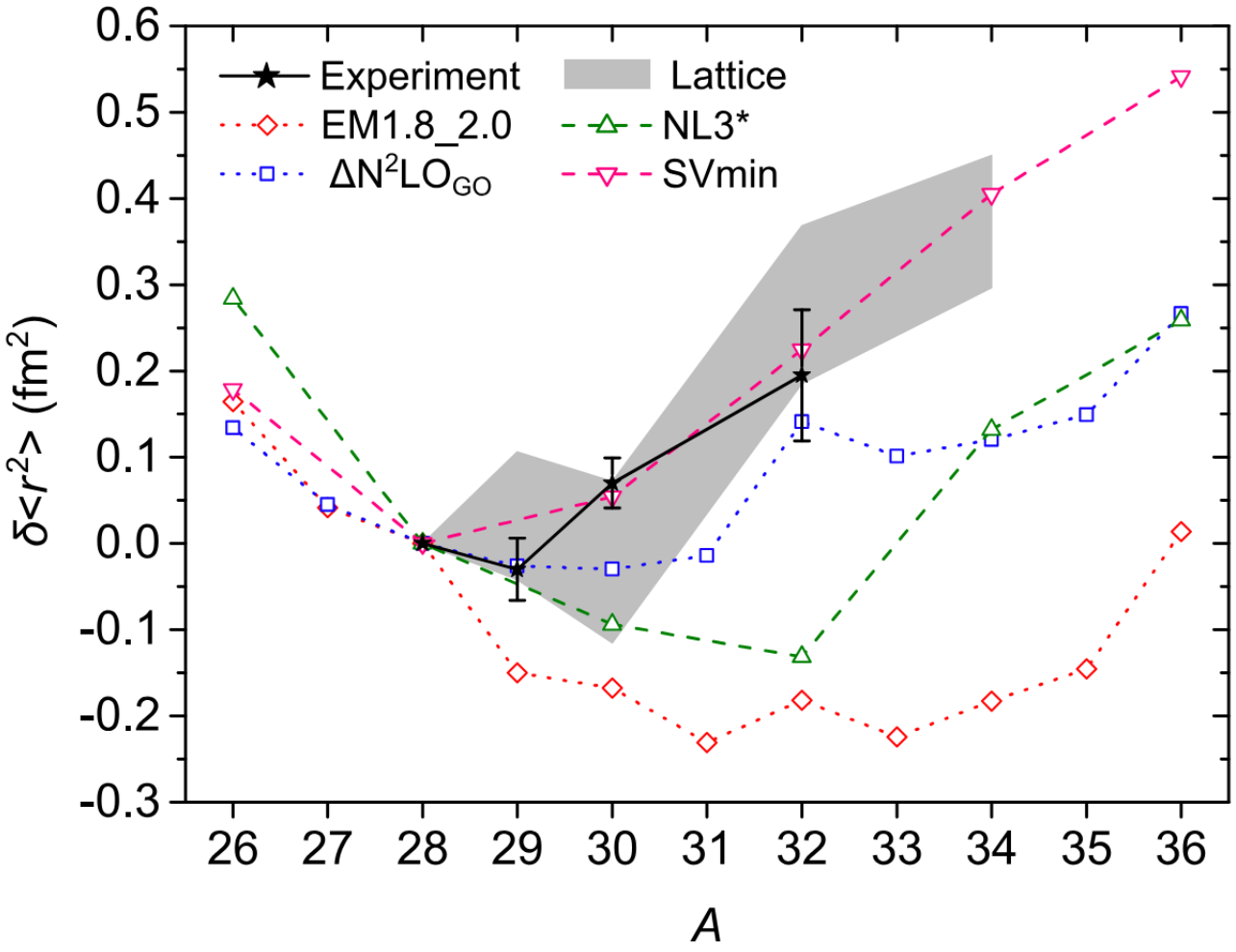

K. König et al., PRL 132, 162502 (2024)

Lattice calculations by Y. Ma

Pinhole algorithm

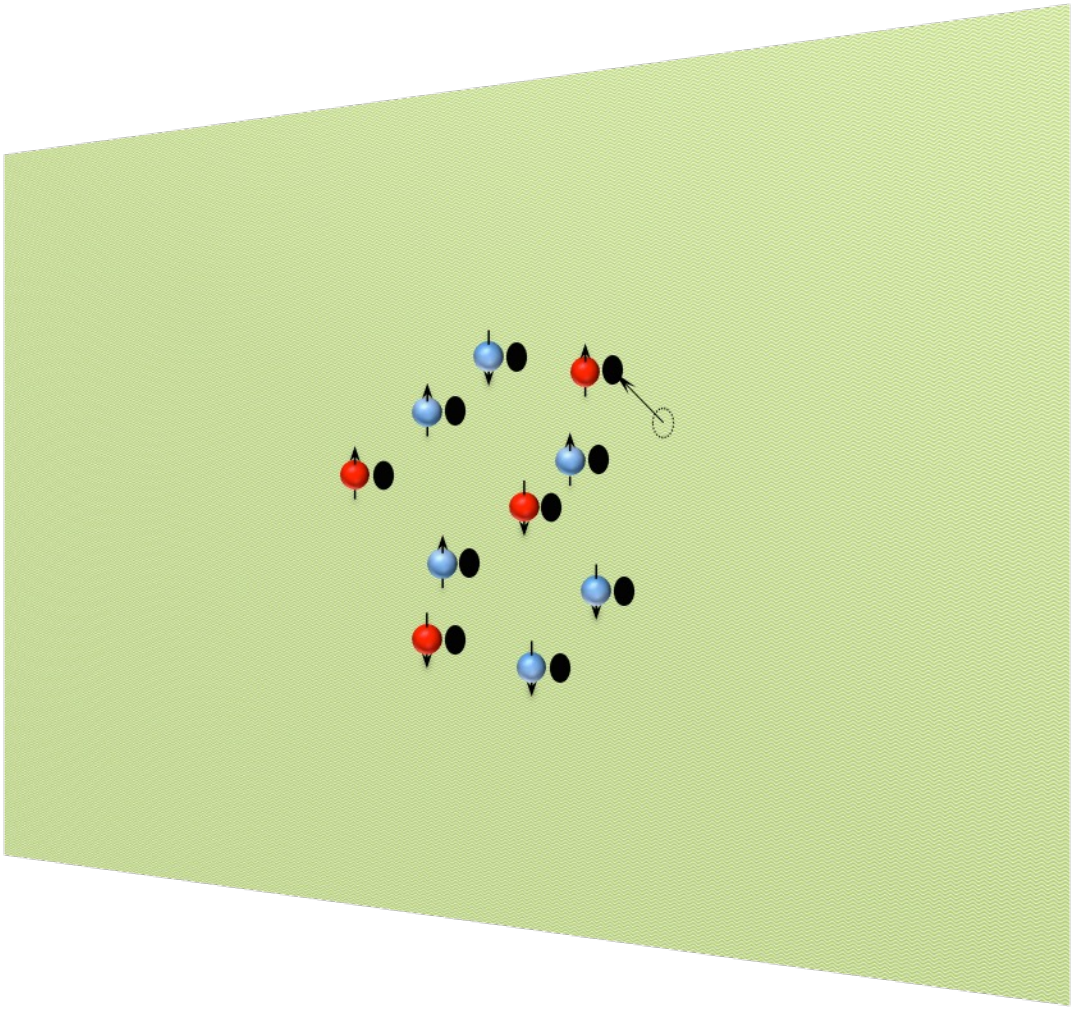

Elhatisari, Epelbaum, Krebs, Lähde, D.L., Li, Lu, Meißner, Rupak, PRL 119, 222505 (2017)

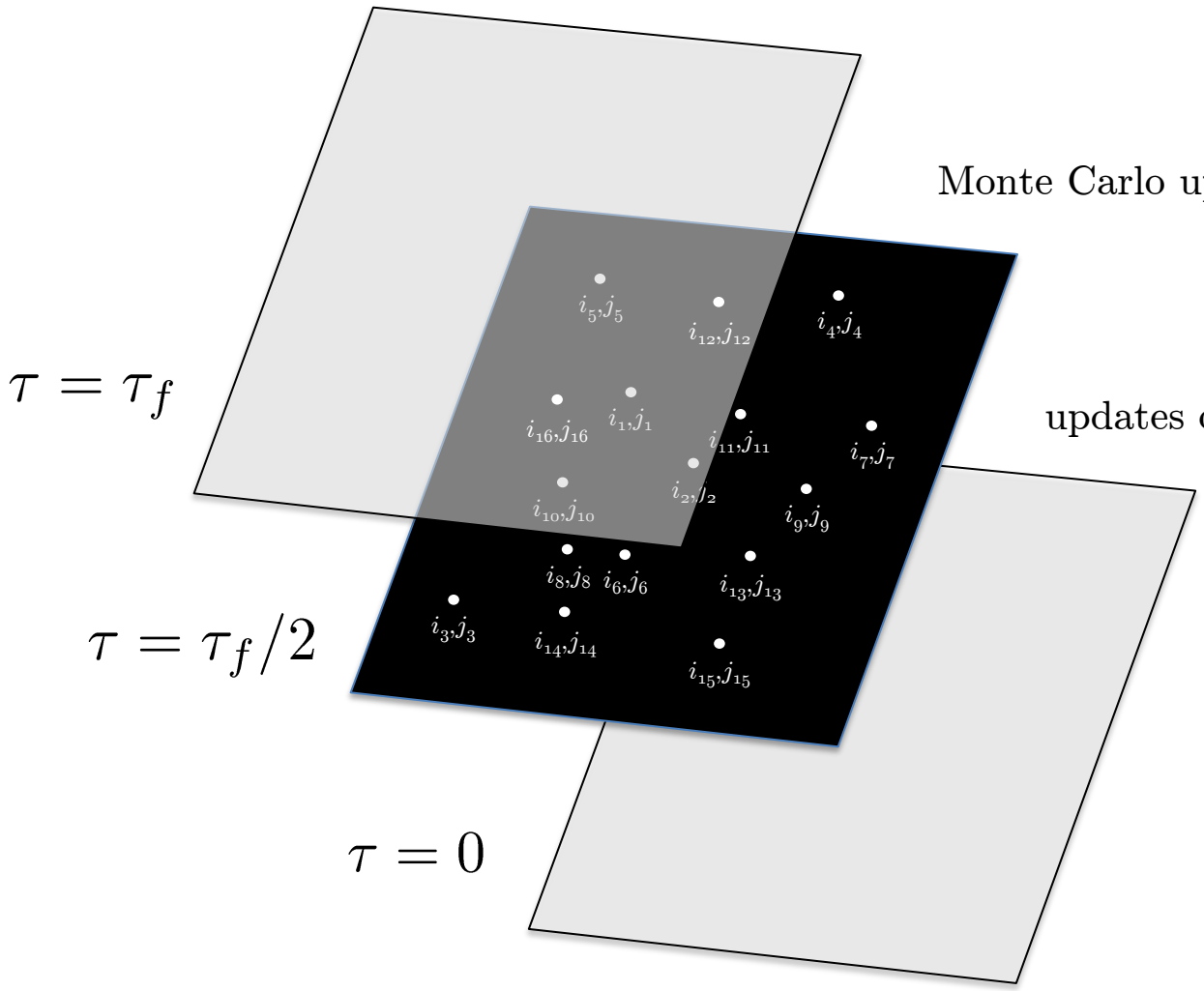

Monte Carlo updates of pinholes

Monte Carlo
updates of auxiliary/pion fields

Elhatisari, Epelbaum, Krebs, Lähde, D.L., Li, Lu, Meißner, Rupak, PRL 119, 222505 (2017)

^{16}O

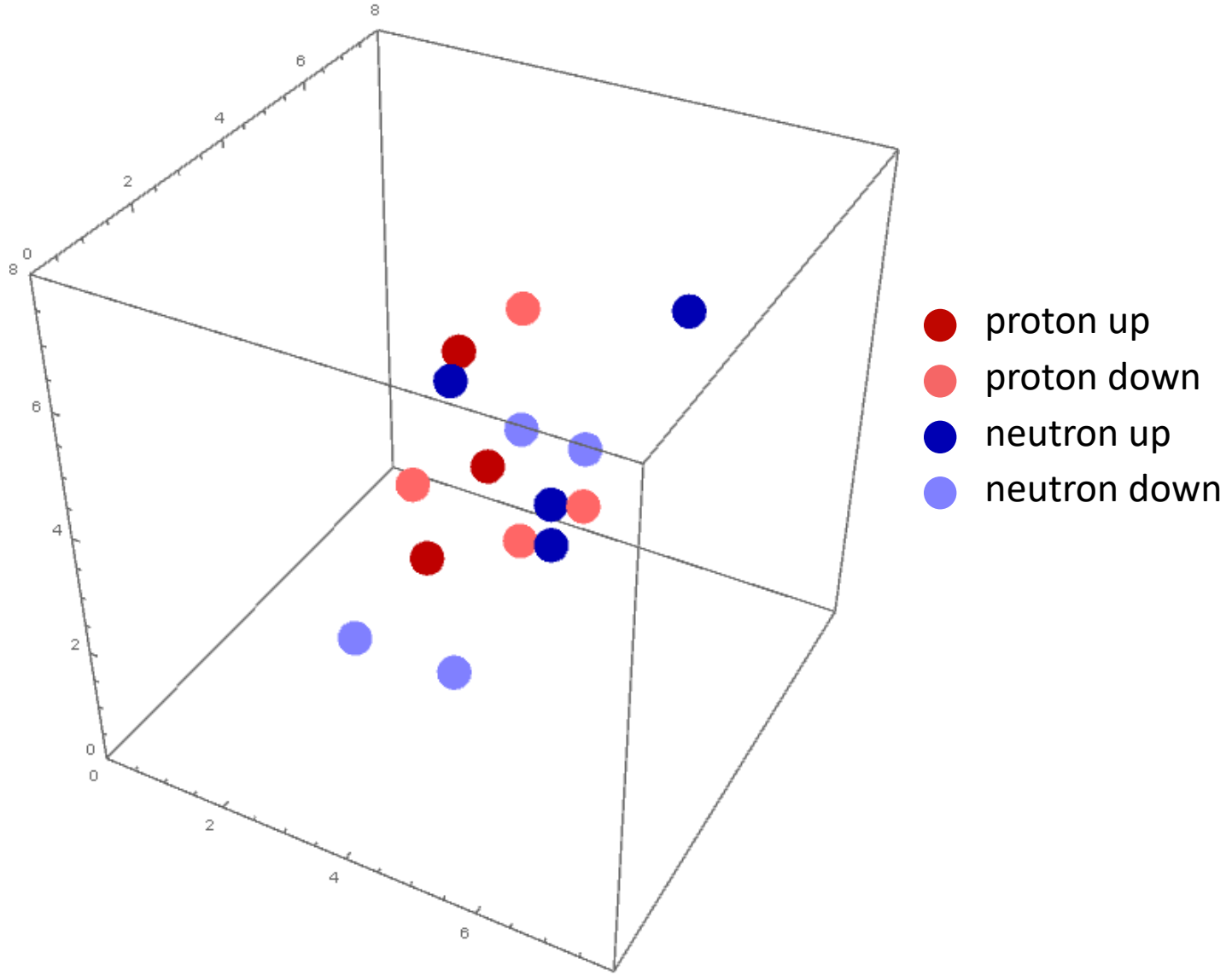

Summerfield, Lu, Plumberg, D.L., Noronha-Hostler, Timmins, Phys. Rev. C 104 L041901 (2021)

Relativistic heavy collisions: ^{16}O^{16}O versus ^{20}Ne^{20}Ne

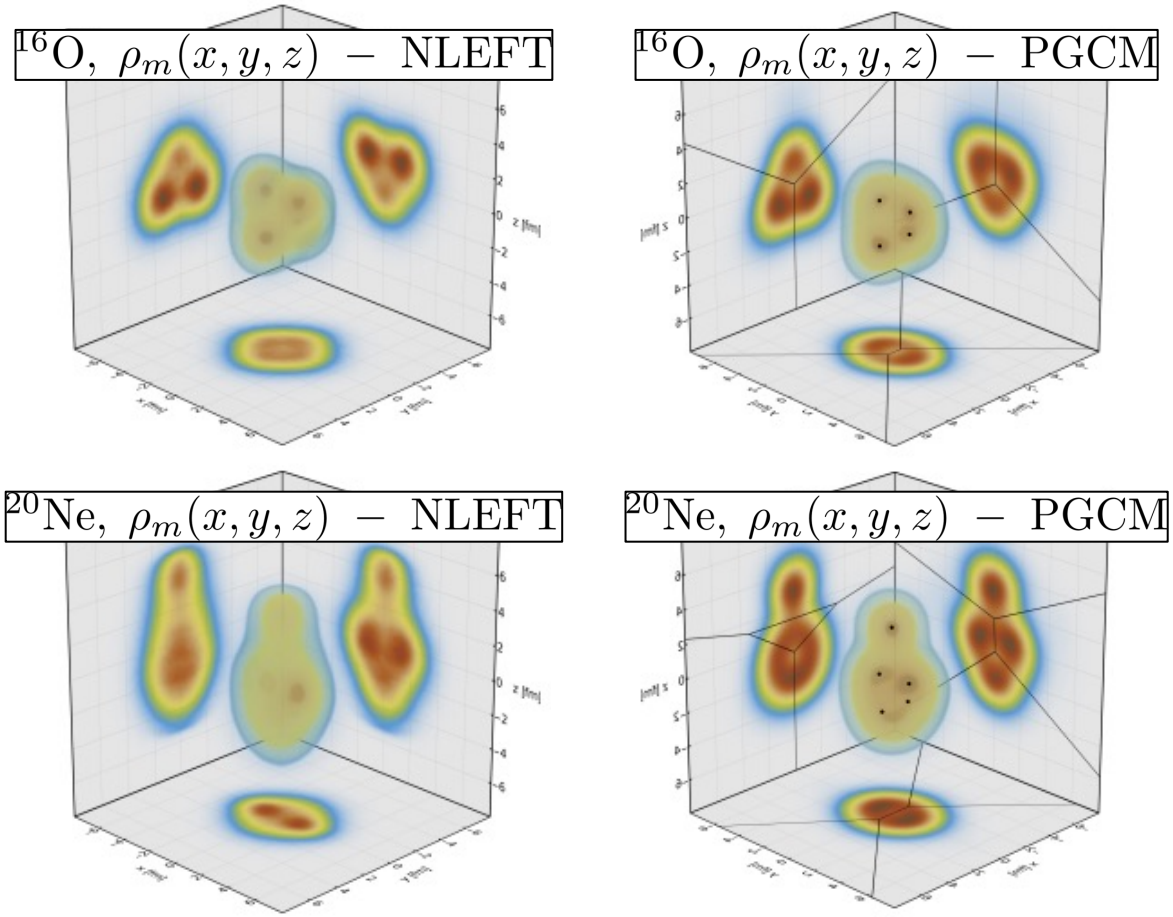

Giacalone et al., arXiv:2402.05995

For the 1% most central events, the elliptic flow of ^{20}Ne^{20}Ne collisions is enhanced by as much as 1.170(8)stat.(30)syst. for NLEFT and 1.139(6)stat.(39)syst. for PGCM relative to ^{16}O^{16}O collisions.

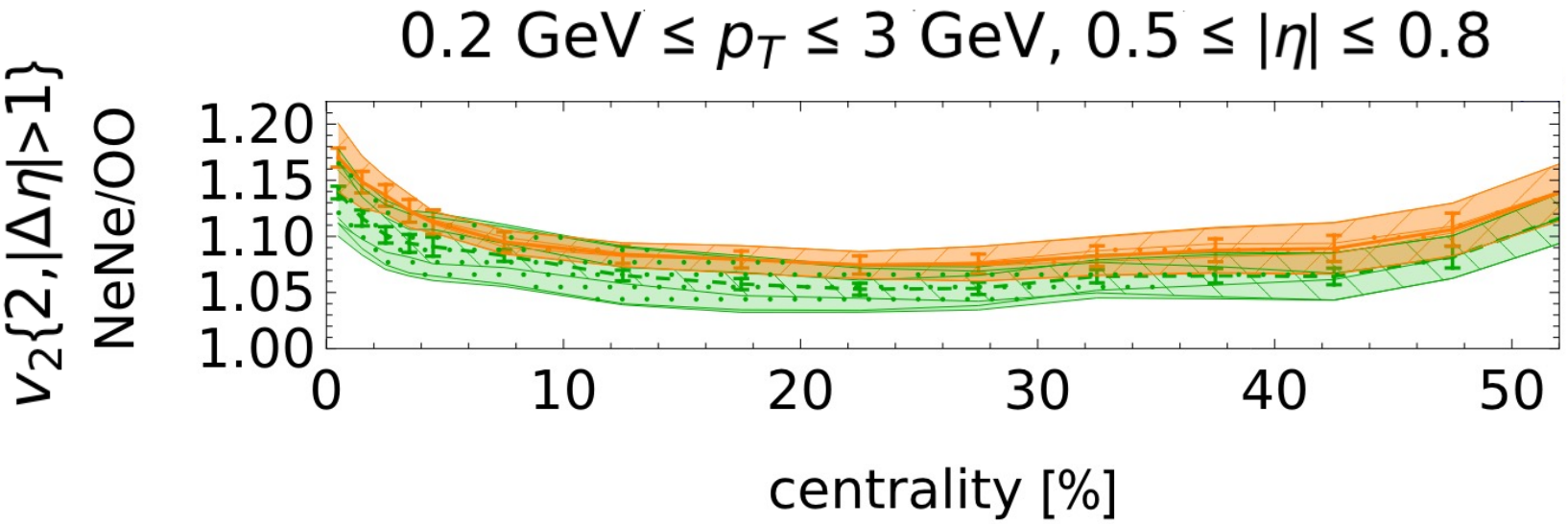

Giacalone et al., arXiv:2402.05995

Asymptotic normalization coefficients

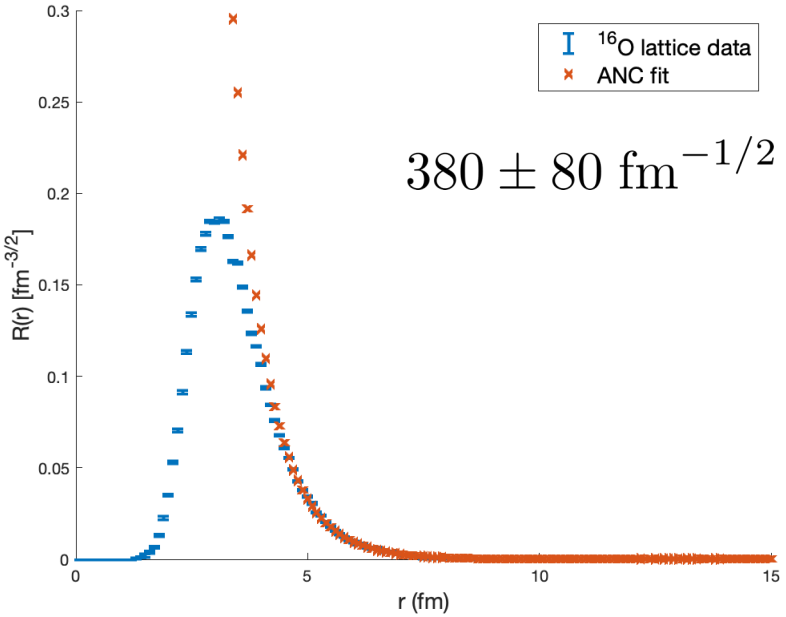

$380 \pm 80\ \mathrm{fm}^{-1/2}$

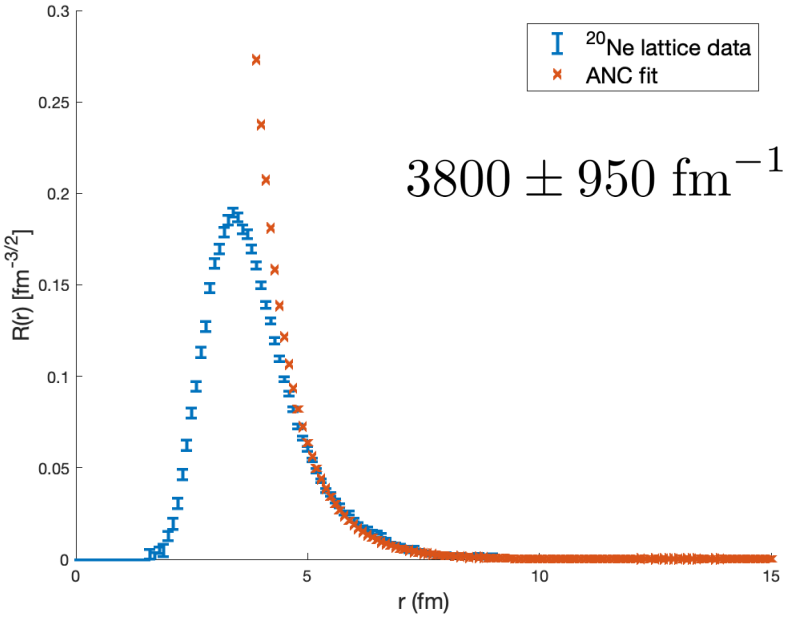

$3800 \pm 950\ \mathrm{fm}^{-1/2}$

$^{12}\mathrm{C}\,(^{20}\mathrm{Ne},^{16}\,\mathrm{O})\,^{16}\mathrm{O}$

E. Harris et al., work in progress

Emergent geometry and duality of ^{12}C

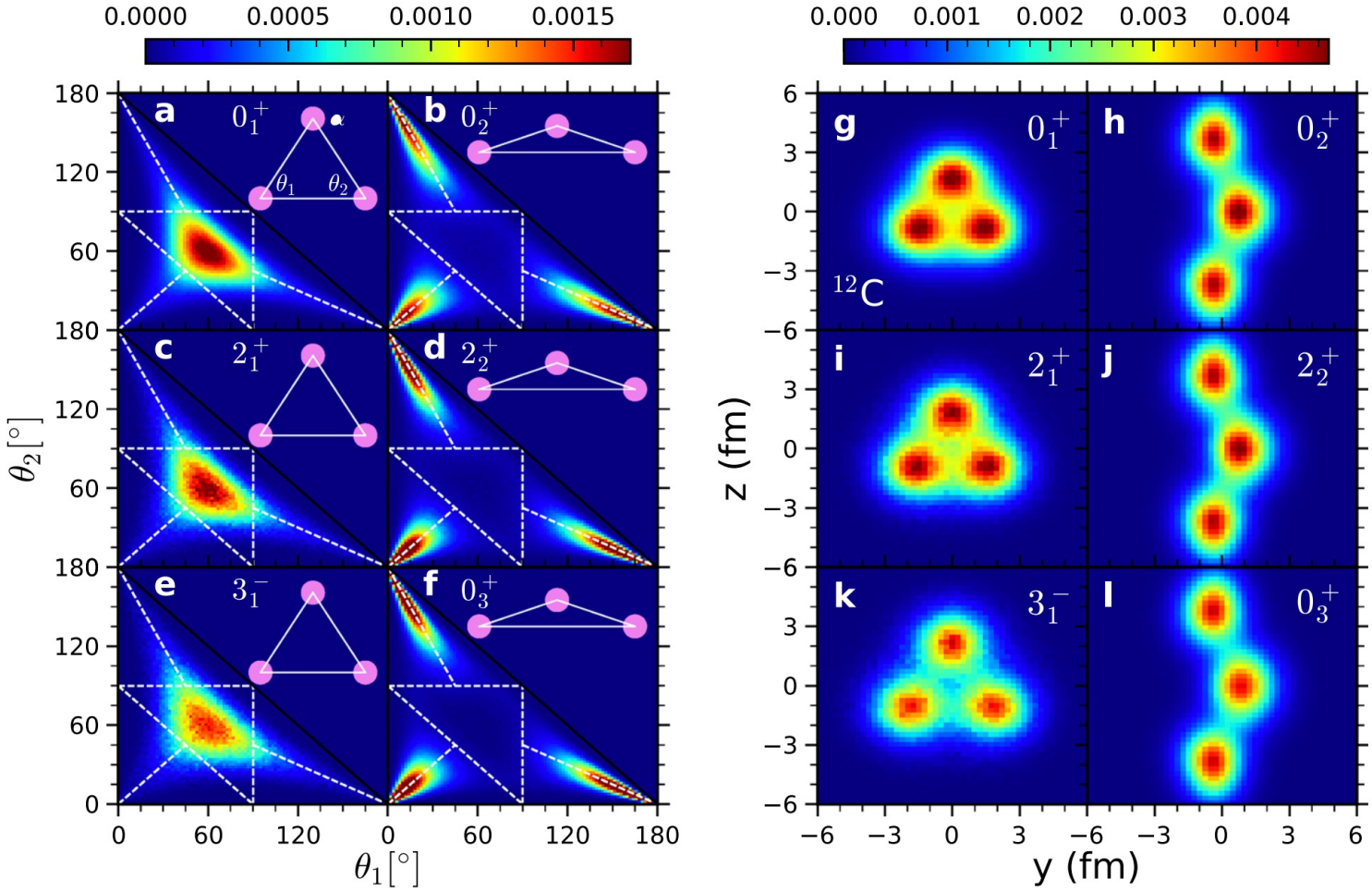

Shen, Elhatisari, Lähde, D.L., Lu, Meißner, Nature Commun. 14, 2777 (2023)

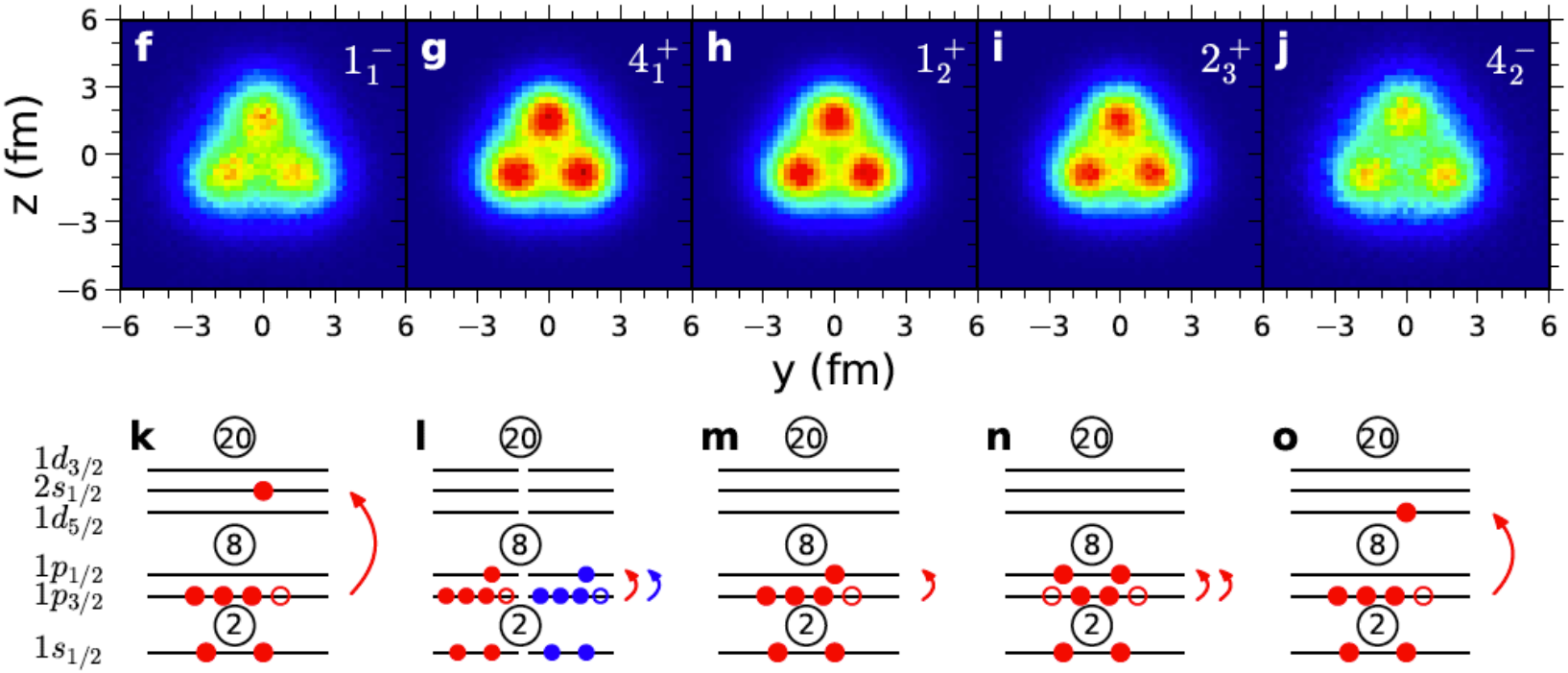
f
1^-_1
g
4^+_1
h
1^+_2
i
2^+_3
j
4^-_2
z (fm)
y (fm)
6
3
0
−3
−6
k
l
m
n
o
20
8
2
$1d_{3/2}$
$2s_{1/2}$
$1d_{5/2}$
$1p_{1/2}$
$1p_{3/2}$
$1s_{1/2}$

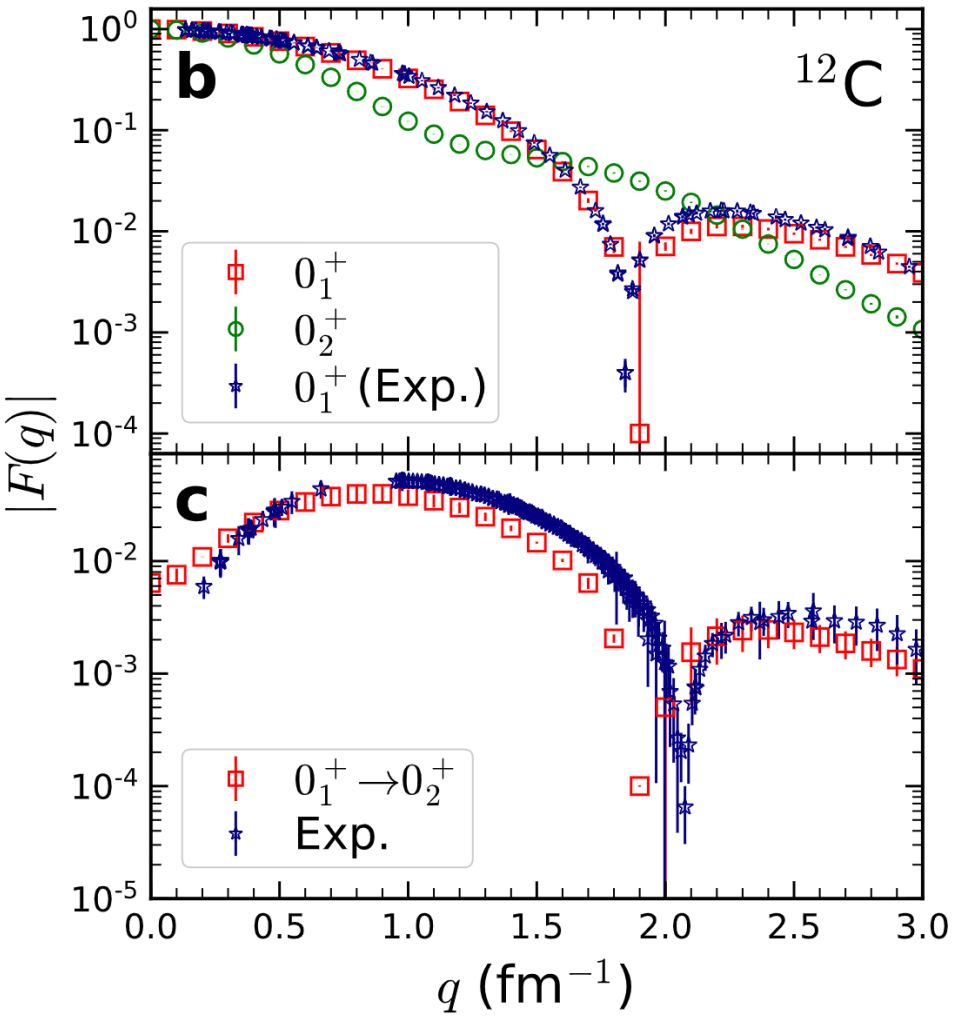

Shen, Elhatisari, Lähde, D.L., Lu, Meißner, Nature Commun. 14, 2777 (2023)

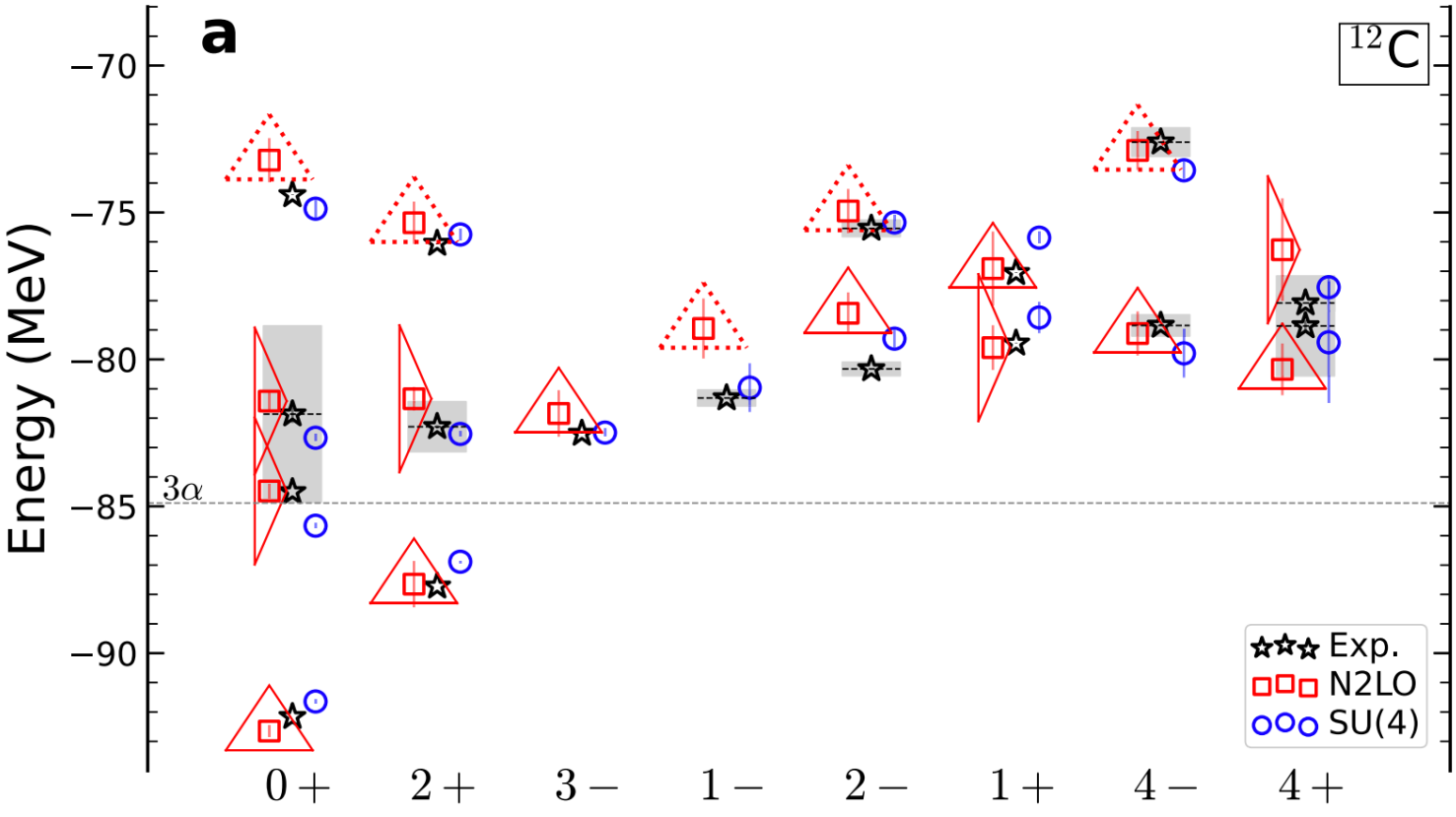

Shen, Elhatisari, Lähde, D.L., Lu, Meißner, Nature Commun. 14, 2777 (2023)

Isotopes of beryllium

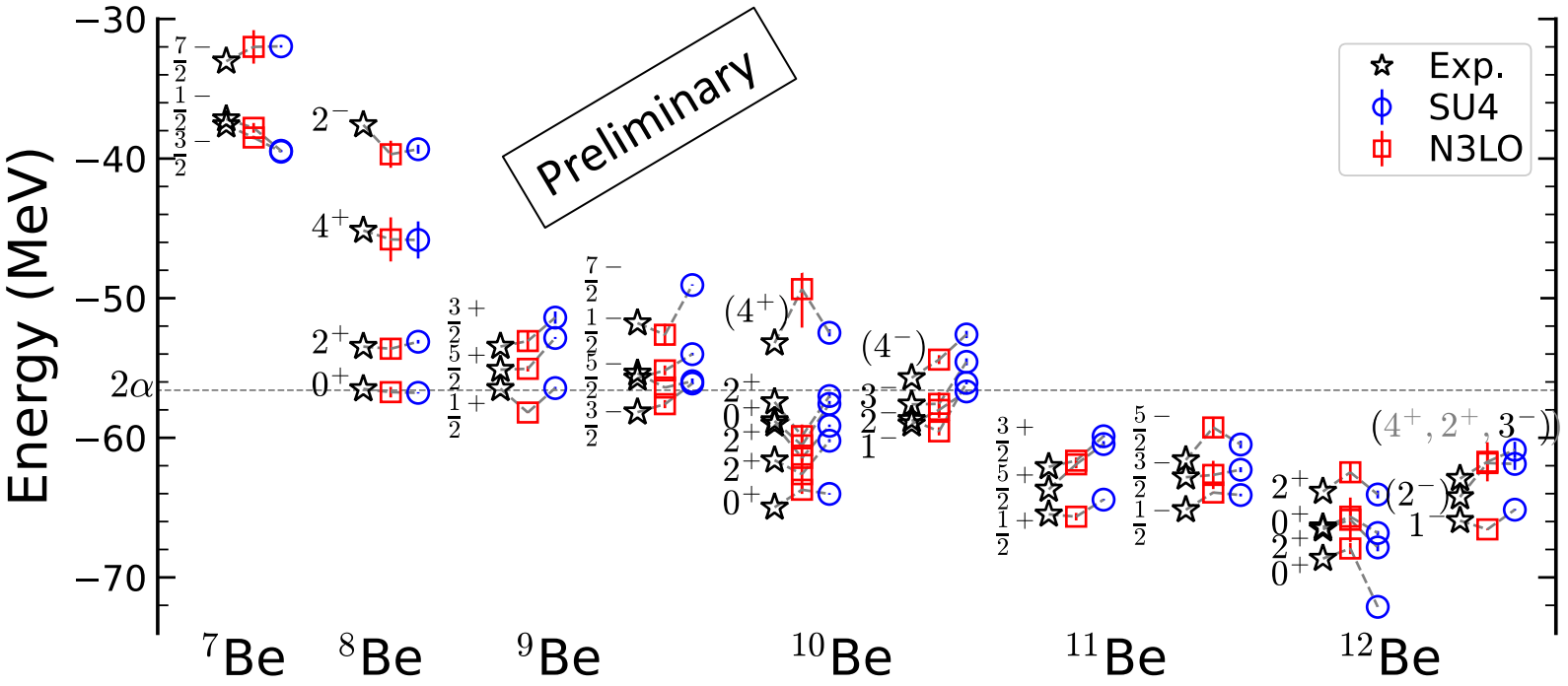

S. Shen, et al., work in progress

Isotopes of beryllium

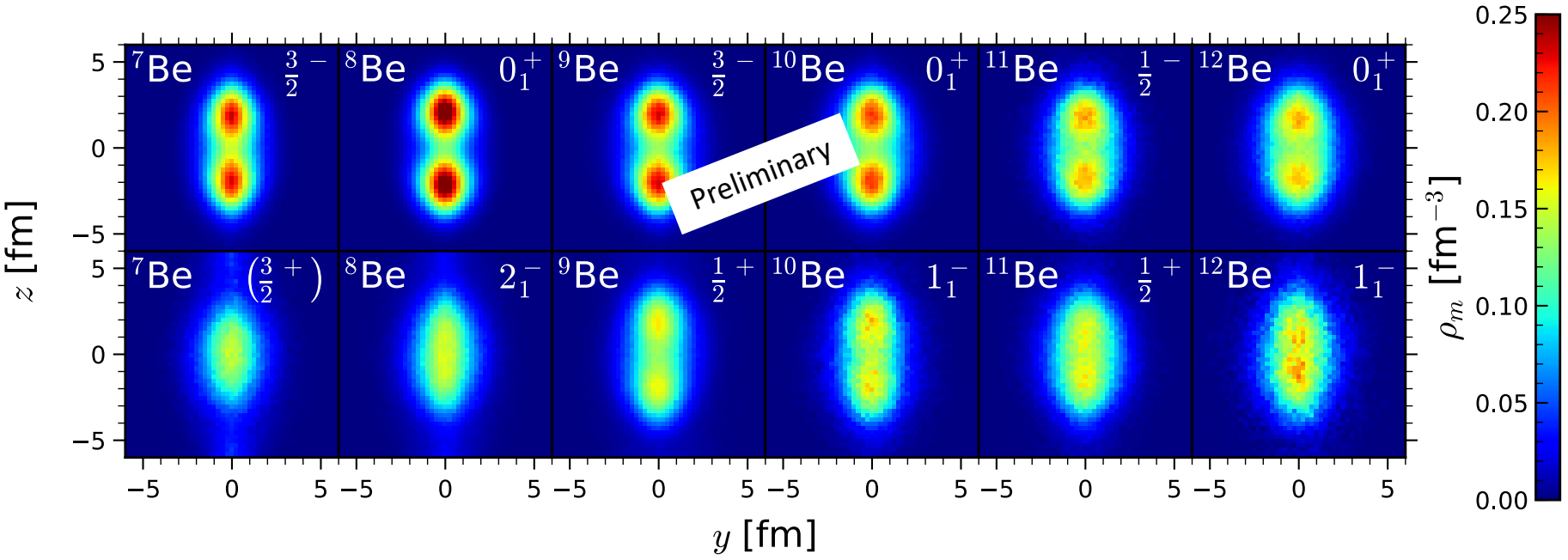

S. Shen, et al., work in progress

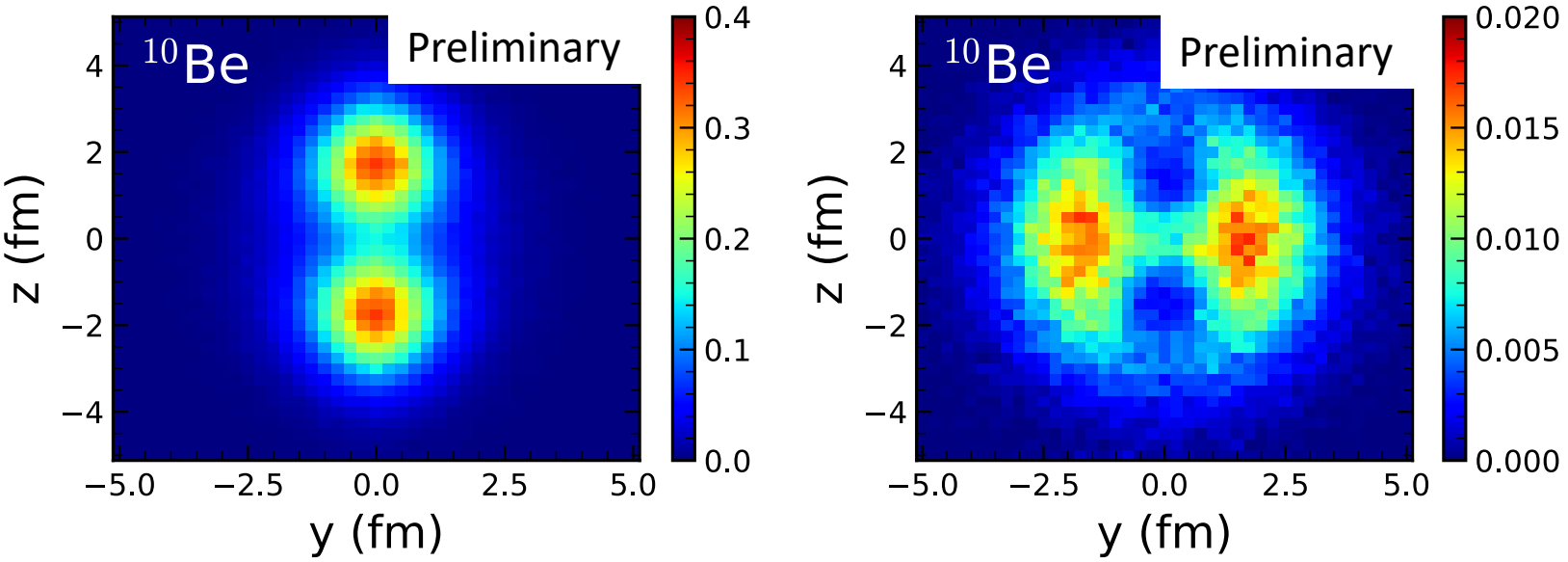

The left panel shows the intrinsic shape of the total nucleon density for ^{10}Be. The right panel shows the density distribution of the two neutrons furthest away from the protons in ^{10}Be.

S. Shen, et al., work in progress

Isotopes of carbon and oxygen

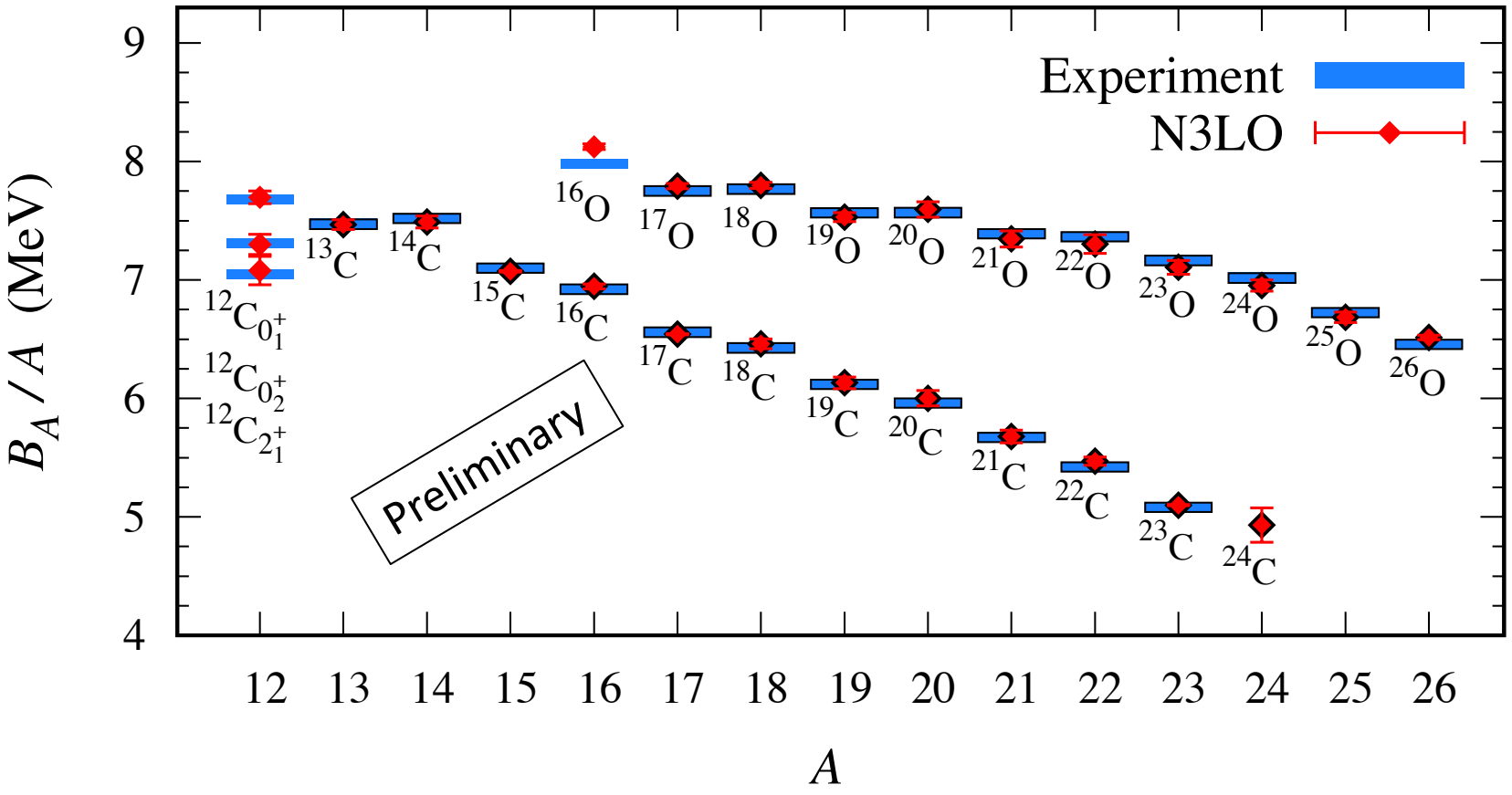

M. Kim, Song, Y. Kim, et al., work in progress

Isotopes of carbon

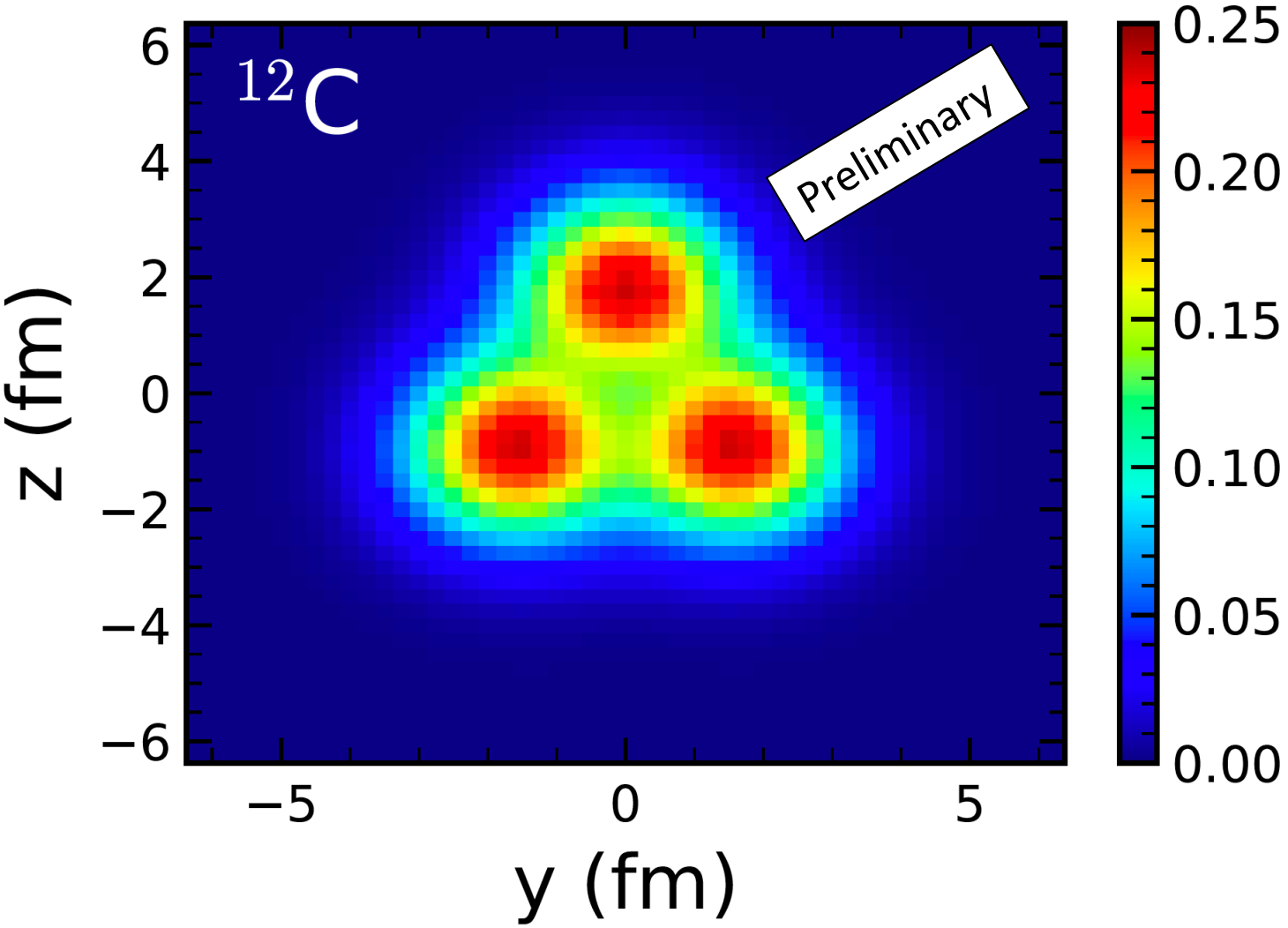

S. Shen, et al., work in progress

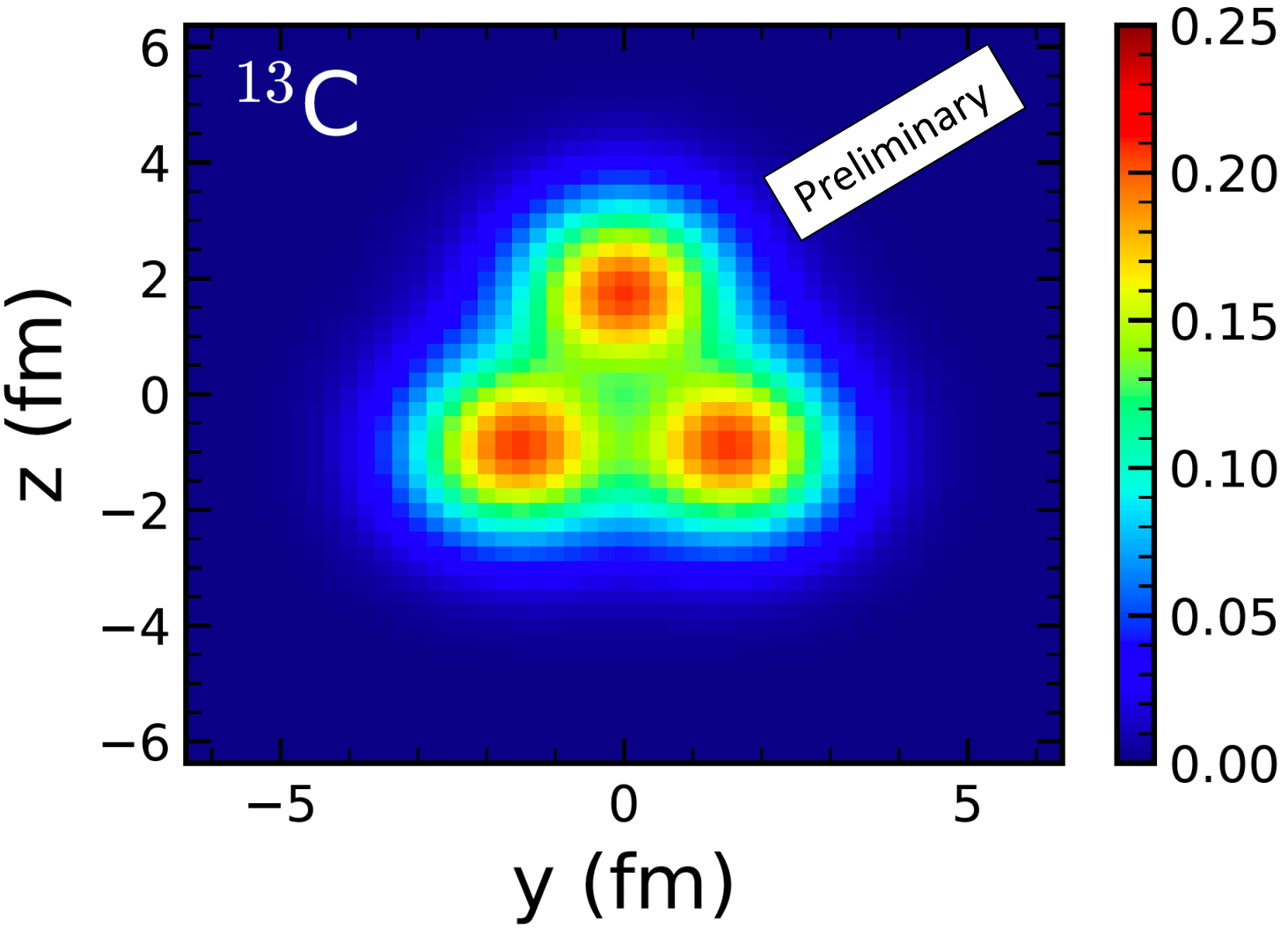
^{13}C
Preliminary
z (fm)
y (fm)
6
4
2
0
−2
−4
−6
−5
0
5
0.25
0.20
0.15
0.10
0.05
0.00

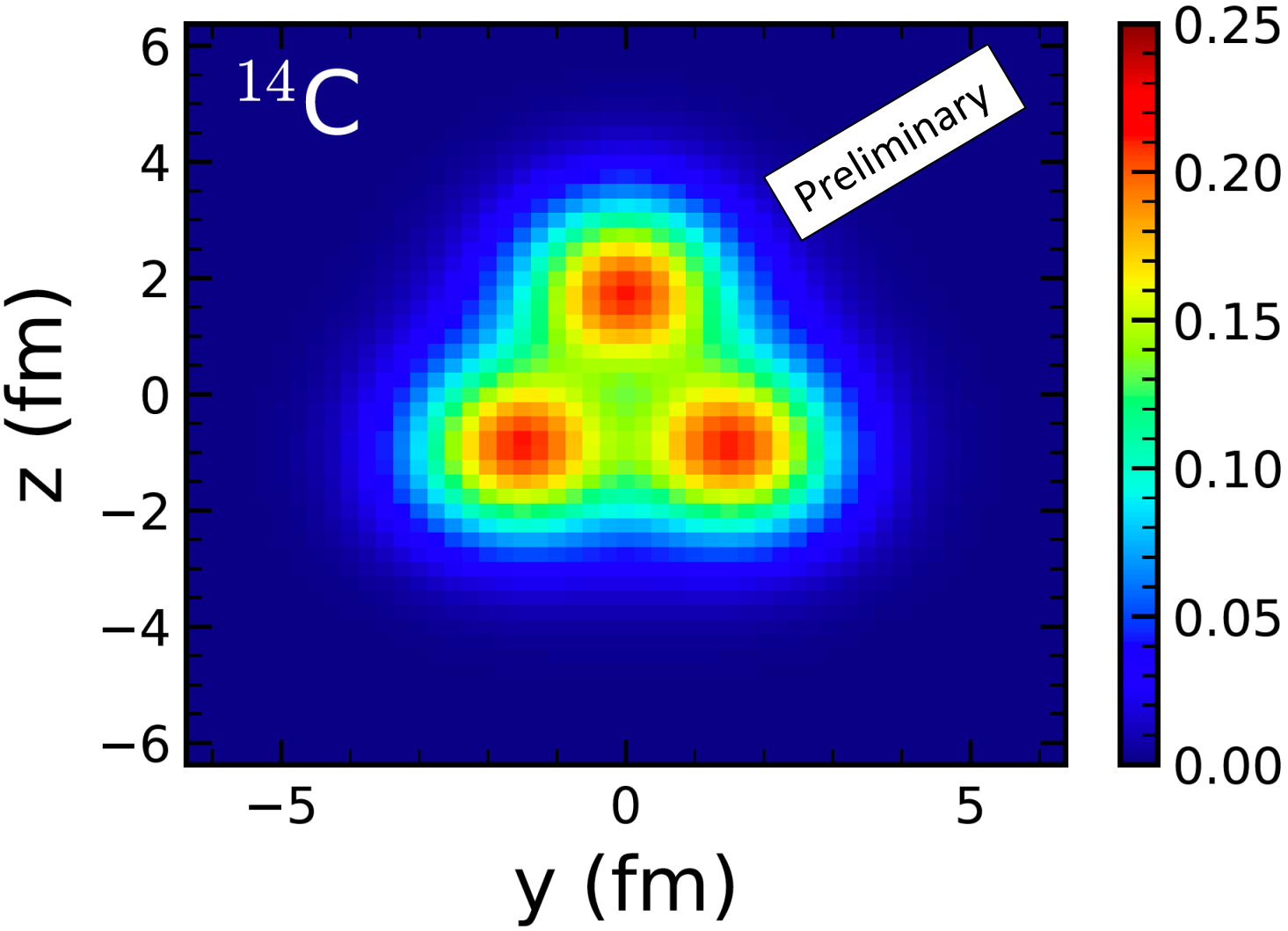
^{14}C
Preliminary
z (fm)
y (fm)
6
4
2
0
−2
−4
−6
−5
0
5
0.25
0.20
0.15
0.10
0.05
0.00

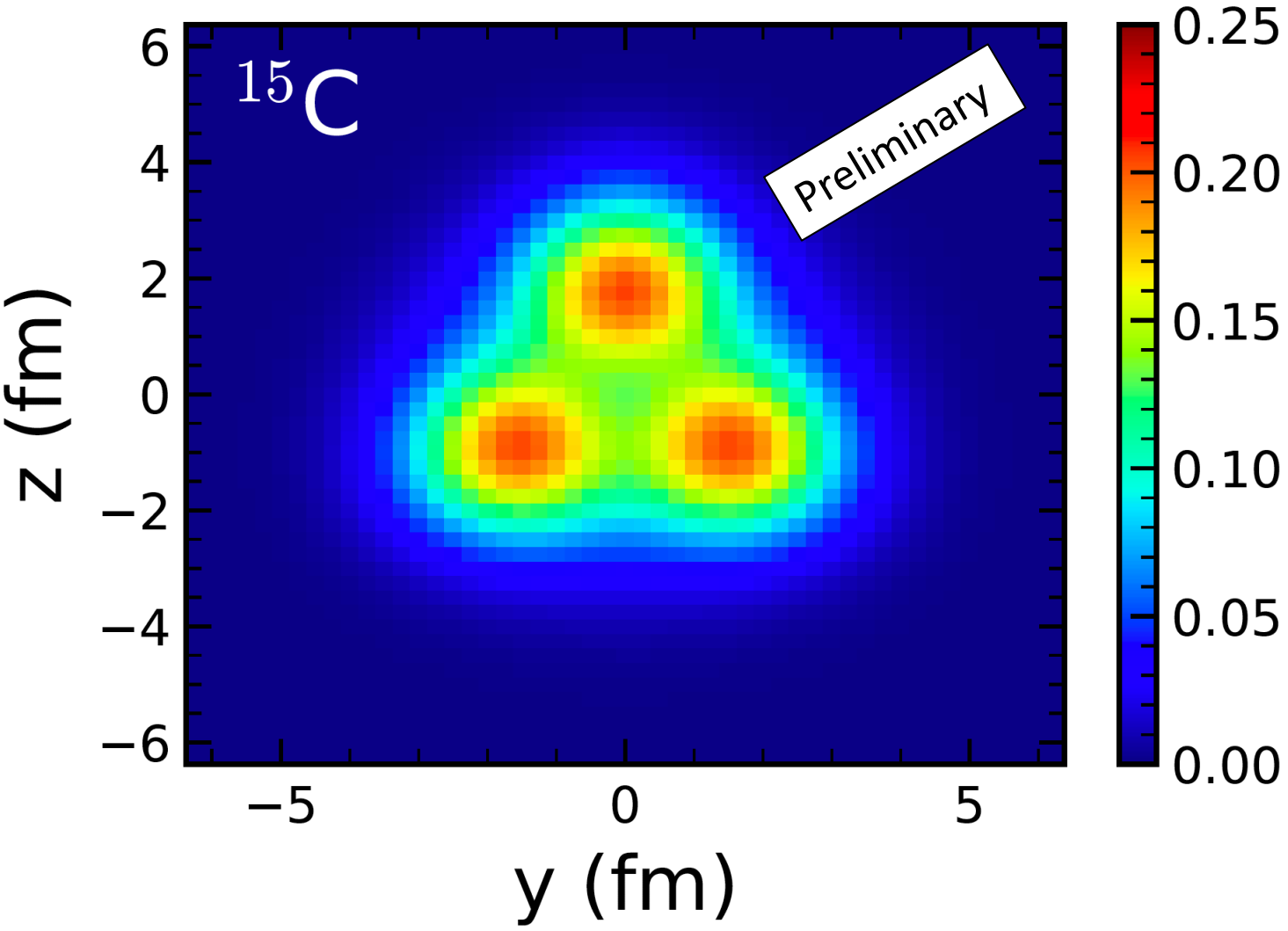
^{15}C
Preliminary
z (fm)
y (fm)
6
4
2
0
−2
−4
−6
−5
0
5
0.25
0.20
0.15
0.10
0.05
0.00

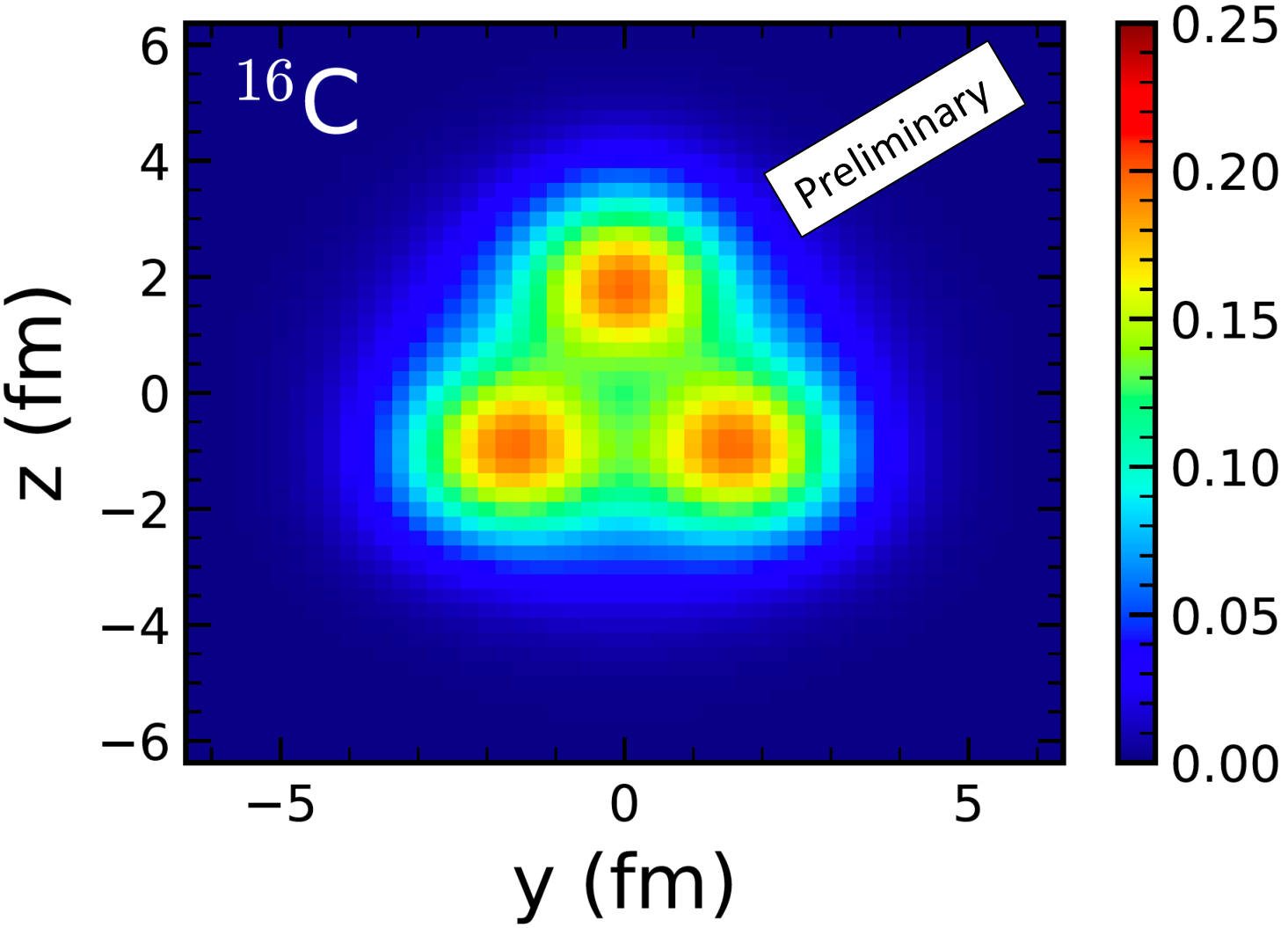
^{16}C
Preliminary
z (fm)
y (fm)
6
4
2
0
−2
−4
−6
−5
0
5
0.25
0.20
0.15
0.10
0.05
0.00

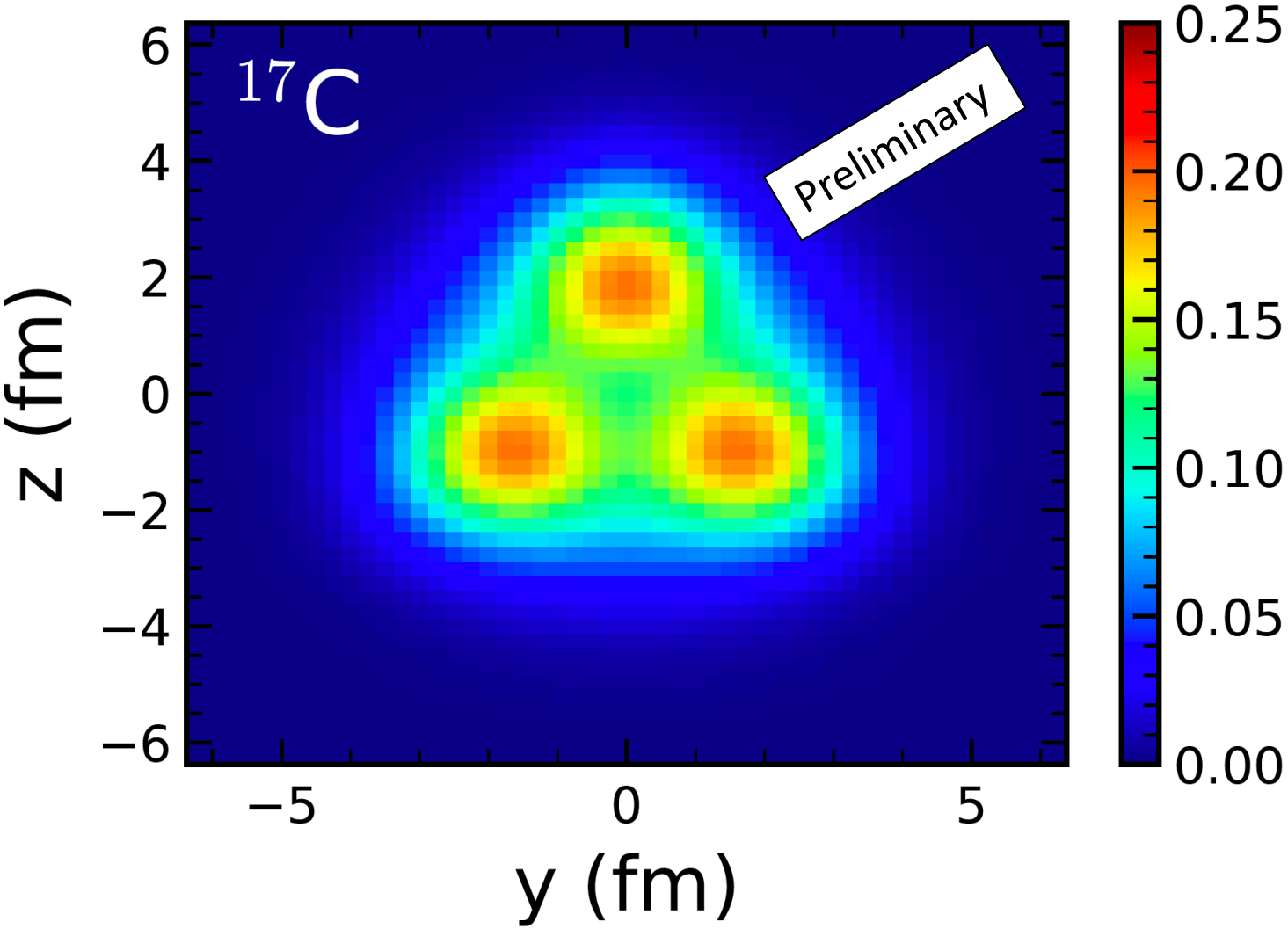
^{17}C
Preliminary
z (fm)
y (fm)
6
4
2
0
−2
−4
−6
−5
0
5
0.25
0.20
0.15
0.10
0.05
0.00

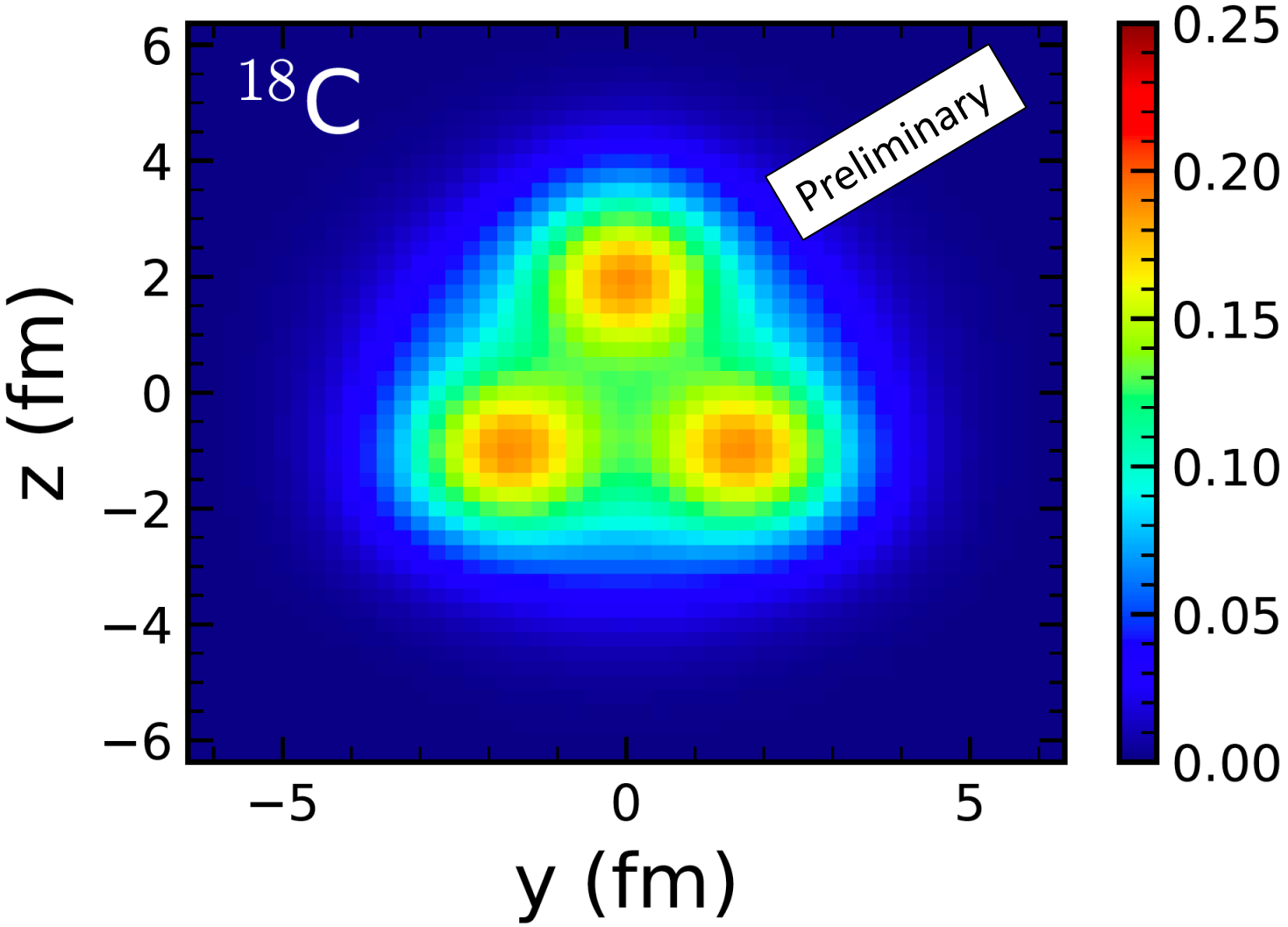
^{18}C
Preliminary
z (fm)
y (fm)
6
4
2
0
−2
−4
−6
−5
0
5
0.25
0.20
0.15
0.10
0.05
0.00

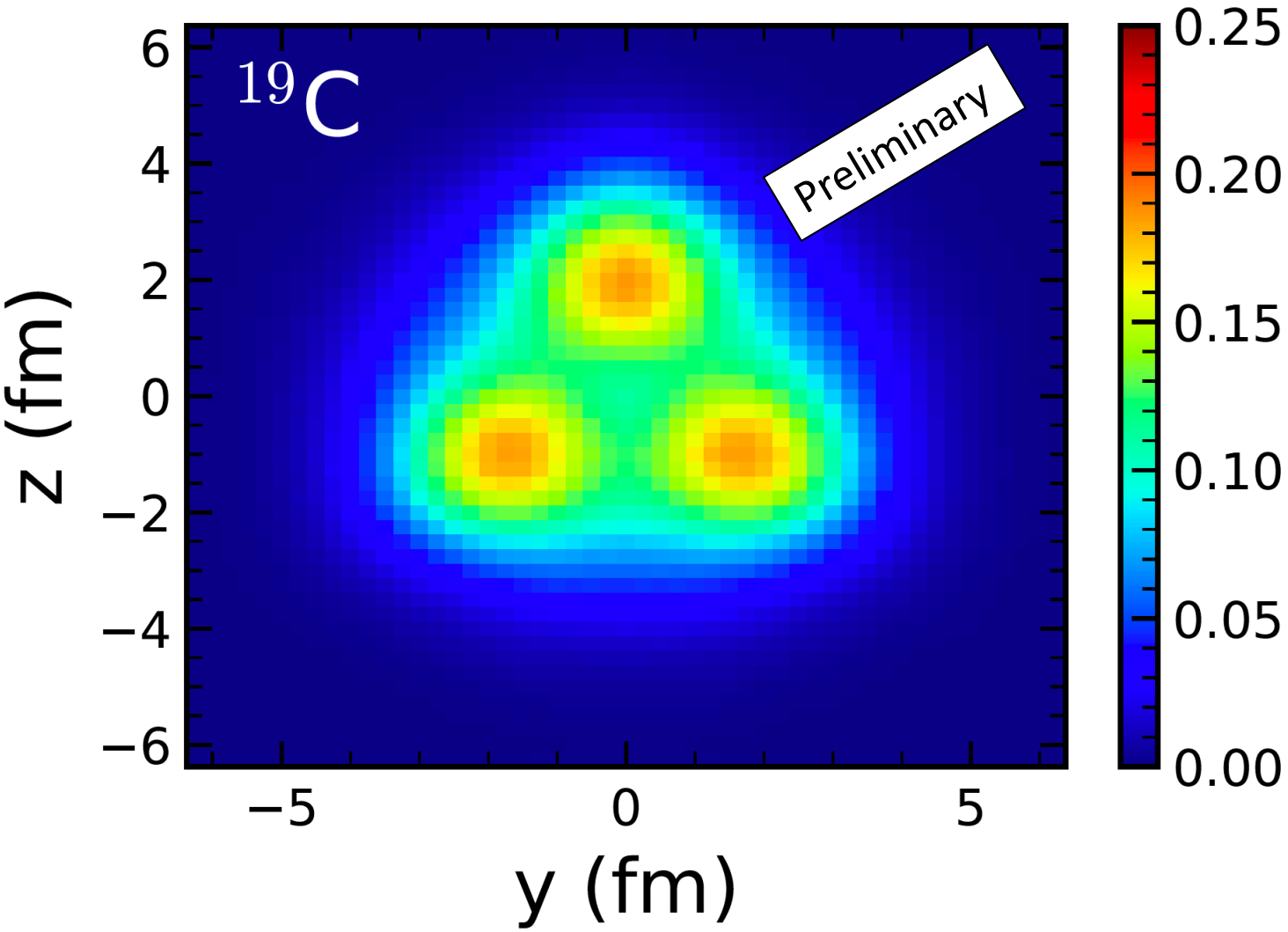
^{19}C
Preliminary
z (fm)
y (fm)
6
4
2
0
−2
−4
−6
−5
0
5
0.25
0.20
0.15
0.10
0.05
0.00

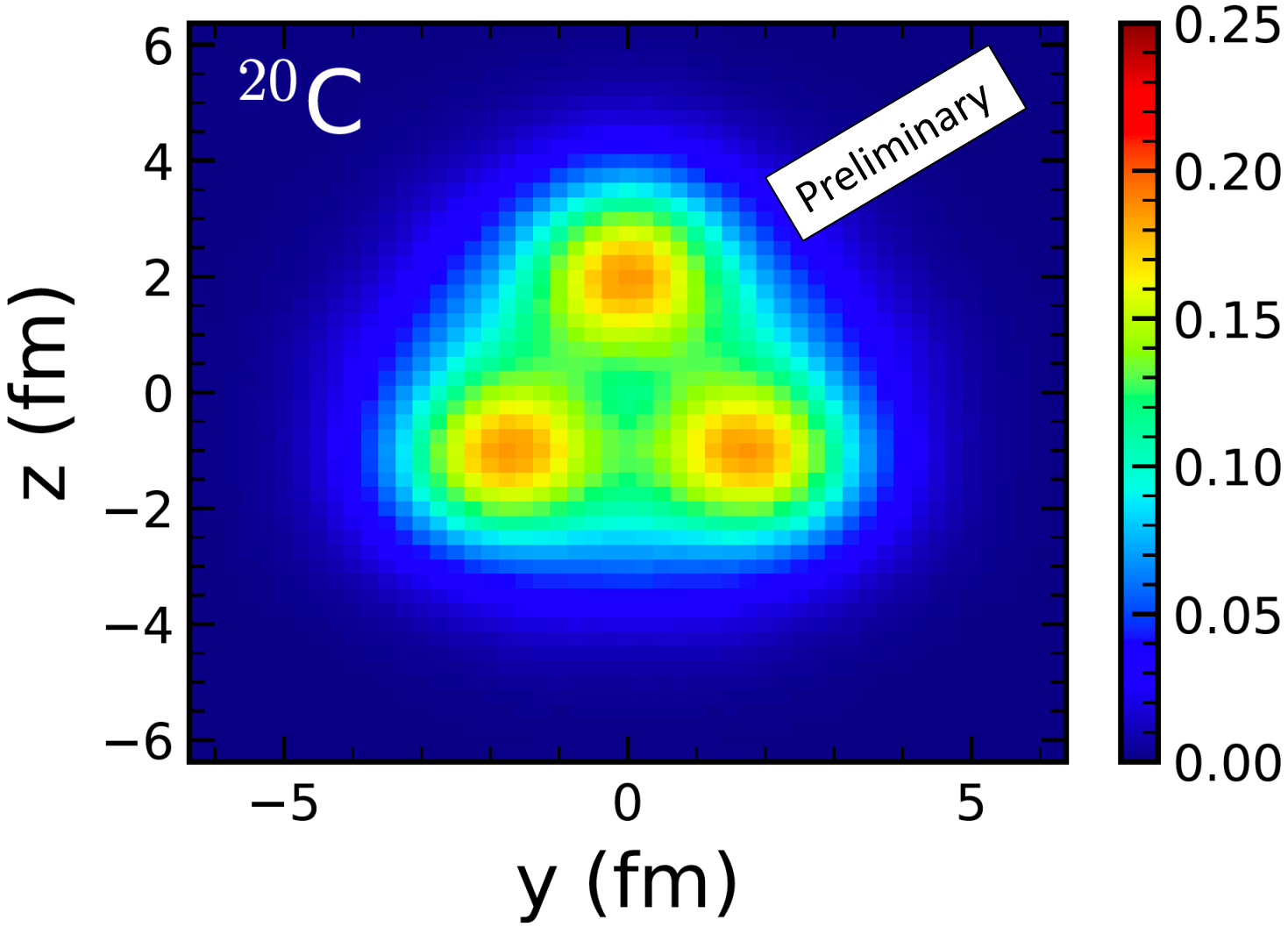
^{20}C
Preliminary
z (fm)
y (fm)
6
4
2
0
−2
−4
−6
−5
0
5
0.25
0.20
0.15
0.10
0.05
0.00

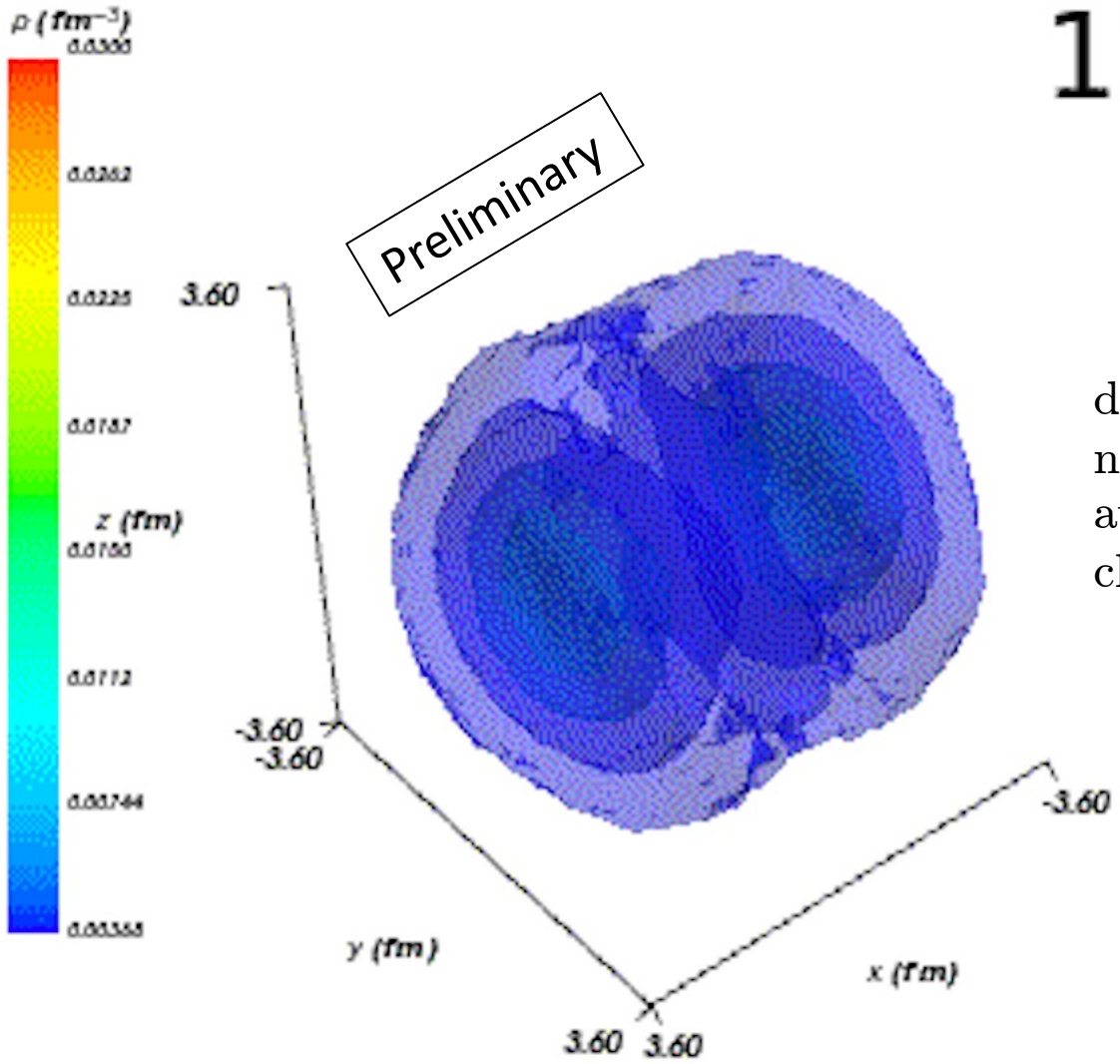

^{13}C

density of the neutron furthest away from its closest proton

S. Shen, et al., work in progress

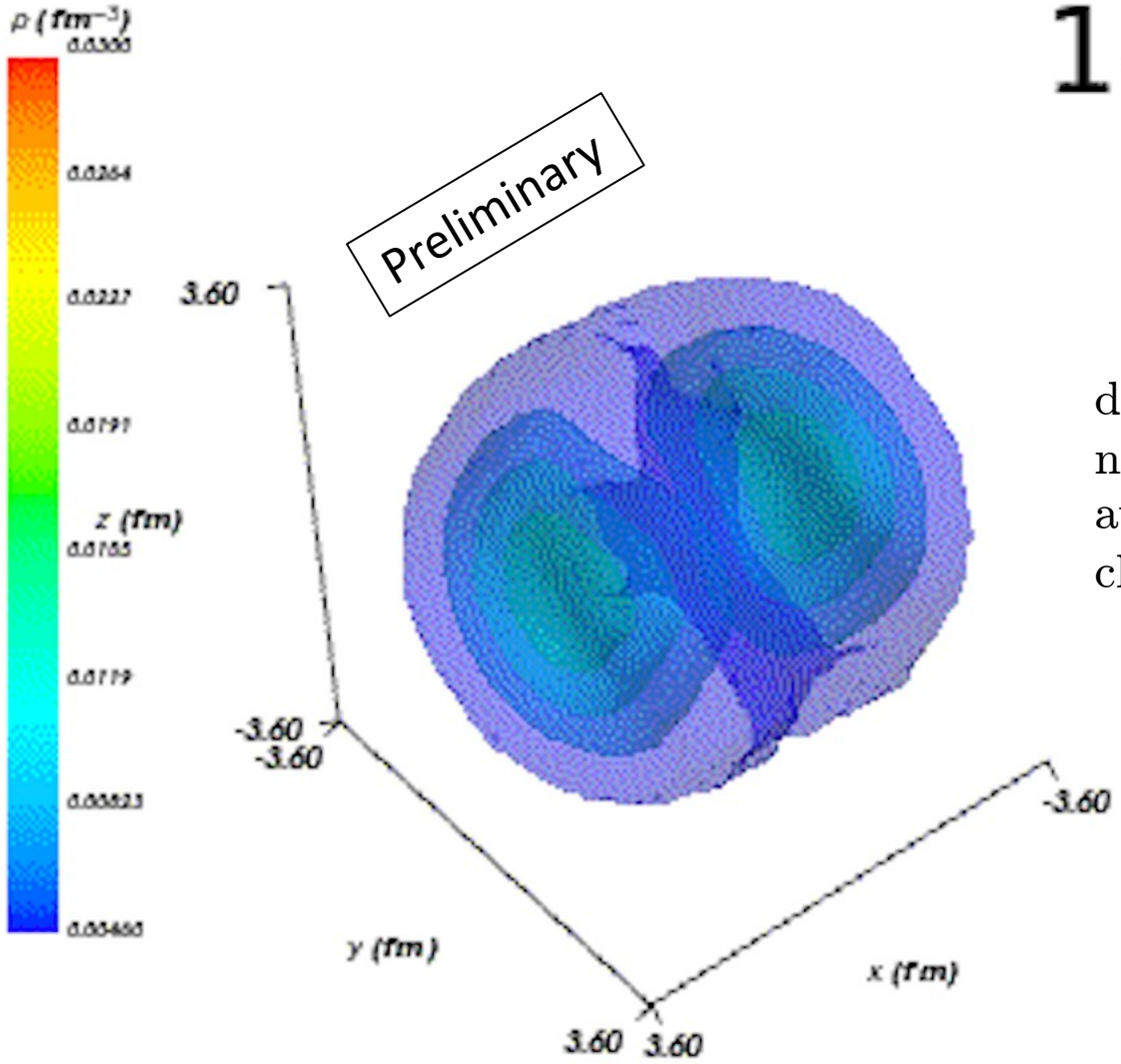

^{14}C

density of the two neutrons furthest away from their closest protons

S. Shen, et al., work in progress

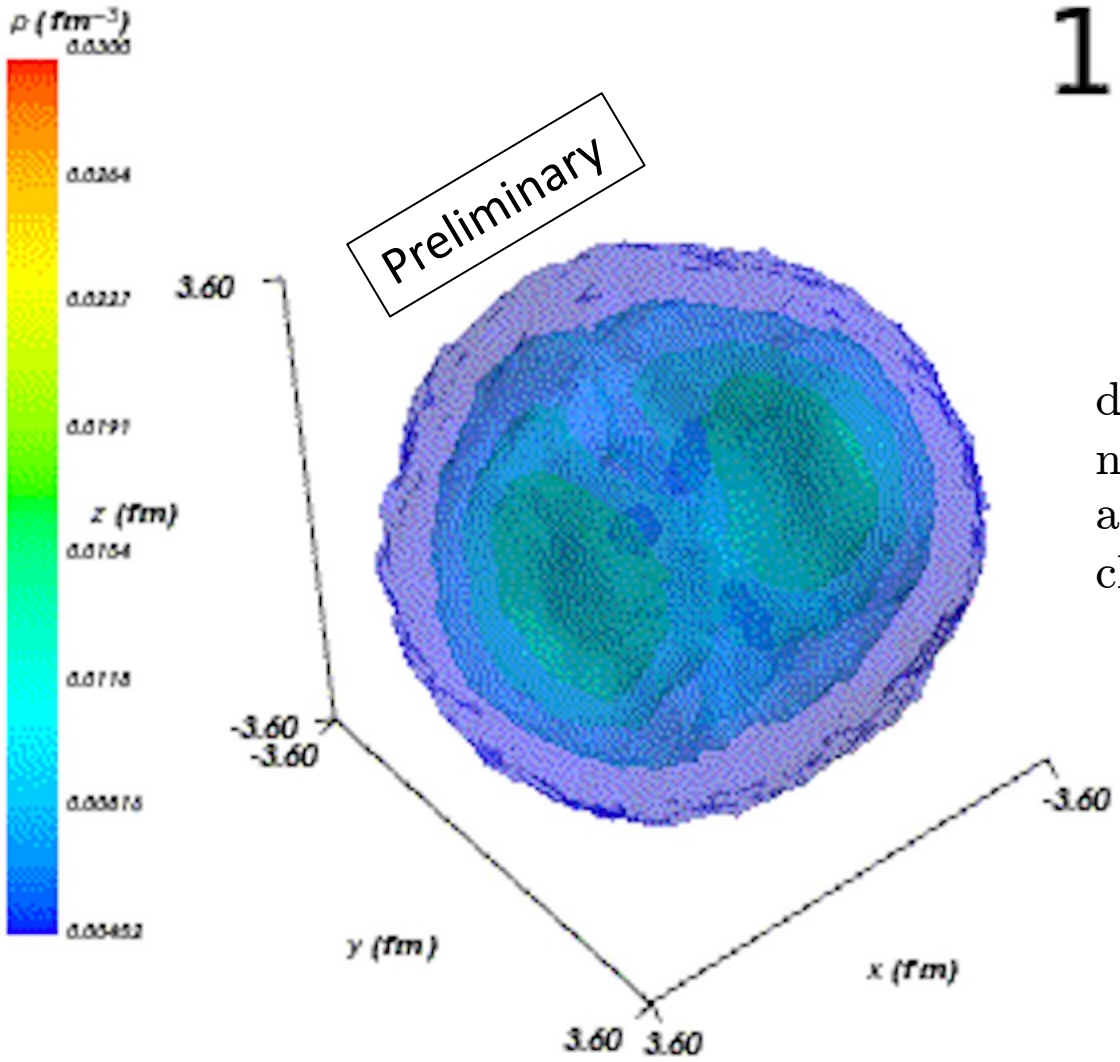

^{15}C

density of the three neutrons furthest away from their closest protons

S. Shen, et al., work in progress

Summary and outlook

Nuclear lattice effective field theory is being used to perform *ab initio* calculations of nuclear structure. Wavefunction matching allows for calculations using high-fidelity chiral effective field theory interactions. The pinhole algorithm allows for detailed studies of nuclear structure correlations, clusters, sizes, and shapes. We are exploring the properties of the beryllium, carbon, and oxygen isotopes.